

Similarities and Differences on the Electronic Structure and Chemical Bonding of Isoelectronic Molecules: X_2NH and HNX_2NH , where $X = N$ and C^-

Georgios A. Tsekouras and Demeter Tzeli*

Cite This: *ACS Omega* 2026, 11, 2976–2990

Read Online

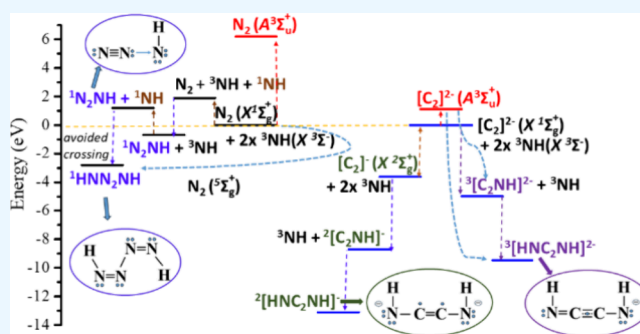
ACCESS |

Metrics & More

Article Recommendations

Supporting Information

ABSTRACT: Identifying similarities and differences among isoelectronic moieties is crucial for understanding chemical bonding, stability, and reactivity. Here, the molecular and electronic structures, chemical bonding, and binding energies of the N_2NH , HNN_2NH , $[C_2NH]^{-/2-}$, and $[HNC_2NH]^{-/2-}$ moieties are calculated via DFT, CCSD(T), QCISD(T), and MRCISD(+Q) methodologies. Although N_2 and $[C_2]^{2-}$ are isoelectronic and both exhibit triple bonds in their ground $X^1\Sigma_g^+$ state and double bonds in their first excited $A^3\Sigma_u^+$ state, their binding energies and stabilities differ. These variations, along with the metastable nature of $[C_2]^{2-}$, affect the bonding and energetics of the studied species. Thus, the N_3H and N_4H_2 molecules have singlet ground states, while the $[C_2NH]^{2-}$ and $[C_2N_2H_2]^{2-}$ anions present triplet ground states. The $N\equiv N-NH$ is formed via a dative bond from $N_2(X^1\Sigma_g^+)$ to $NH(a^1\Delta)$, while adding another NH , the bonding changes to $HN=N-N=NH$; their CCSD(T) formation energies are -2.59 eV (N_2NH) and -11.93 eV (HNN_2NH). On the contrary, in both $[C_2NH]^{2-}$ and $[HNC_2NH]^{2-}$ anions, electron charge is transferred to NH , i.e., the in situ diatomic moieties are excited states of $[C_2]^-$ and $C_2 + NH^- (X^2\Pi)$. Their formation energies are -1.14 eV ($[C_2NH]^{2-}$) and -8.57 eV ($[HNC_2NH]^{2-}$). Electron transfer from metastable $[C_2]^{2-}$ to one or two NH stabilizes both $[C_2NH]^{2-}$ and $[HNC_2NH]^{2-}$, suggesting their possible experimental detection.



1. INTRODUCTION

Polynitrogens are regarded as promising clean energy storage materials due to their exceptionally high energy content.¹ Thus, the synthesis of a metastable molecular nitrogen allotrope beyond N_2 or compounds including polynitrogens enhances the fundamental understanding of chemistry and may pave the way for novel energy storage technologies in the future.³ Over the last three decades, the demand for sodium azide (NaN_3), which is the principal active ingredient in automobile air bag inflators, has significantly increased, while its accidental environmental releases have also increased.⁴ NaN_3 is readily hydrolyzed to yield hydrazoic acid, also known as hydrogen azide, azic acid, azoimide, or triazirine, HN_3 or N_3H . The azic acid is a volatile substance that is strongly distributed to the gas phase under atmospheric conditions. For instance, even at low concentrations of 6.5 ppm (m/v) NaN_3 in the aqueous phase, the concentration of its hydrolyzed N_3H product in the corresponding gas phase in atmospheric conditions reaches the threshold limit value of 0.11 ppmv.⁵ Thus, it is important to investigate the reactions of the HN_3 product, i.e., its molecular structure and photophysical properties.^{5–7}

The addition of an NH molecule to N_3H can result in the formation of the tetrazetene, N_4H_2 . Theoretical calculations

have shown that both N_3H^{5-8} and $N_4H_2^{69}$ are stable. Their heat of formation, i.e., the formation from the corresponding atoms, was calculated at 453.7 kJ/mol = 4.70 eV and 514.1 kJ/mol = 5.33 eV, at the G2 level of theory.⁶ Tetrazetene, N_4H_2 , is an important molecule because it forms the core structure of tetrazines, which are well-known compounds for their applications in medicinal chemistry, as a drug, and in material science, where they absorb visible light, and they are used in various metal-free catalytic methodologies in organic synthesis and the chemical industry.¹⁰ Thus, the investigation of the electronic structures, bonding, and reactivity of nitrogen-centered radicals attracts the interest of the research community, and a variety of nitrogen-centered radicals have been studied with DFT or high-level correlated methods.^{1–11}

Monoanions of carbon clusters have now been detected by negative ion photoelectron spectroscopy.¹² In 1954, Honig detected the first monoanions, C_2^- , C_3^- , and C_4^- .¹³ The

Received: September 3, 2025

Revised: November 21, 2025

Accepted: December 25, 2025

Published: January 5, 2026



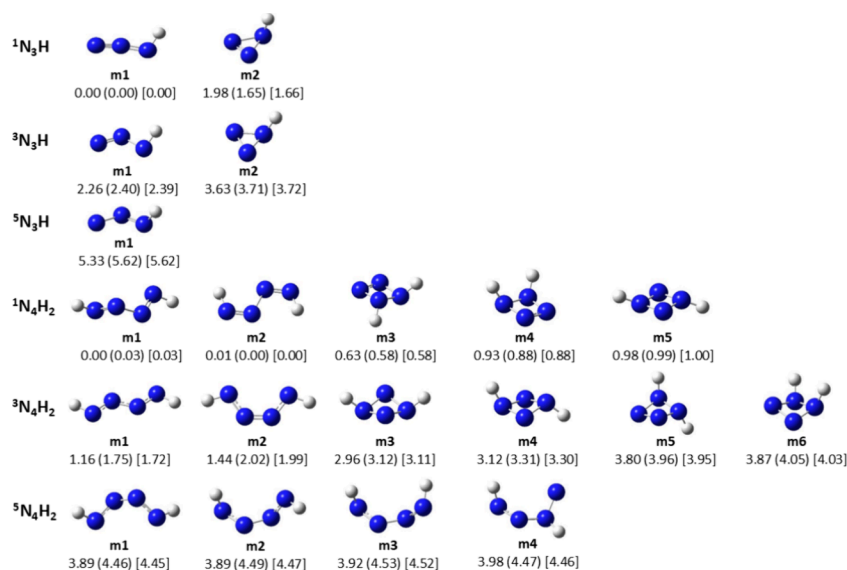


Figure 1. Minimum structures and relative energies in eV of the N_2NH and HNN_2NH molecules at the B3LYP/6–311+G(d,p), (CCSD(T)/aug-cc-pVTZ), and [QCISD(T)/aug-cc-pVTZ] methods.

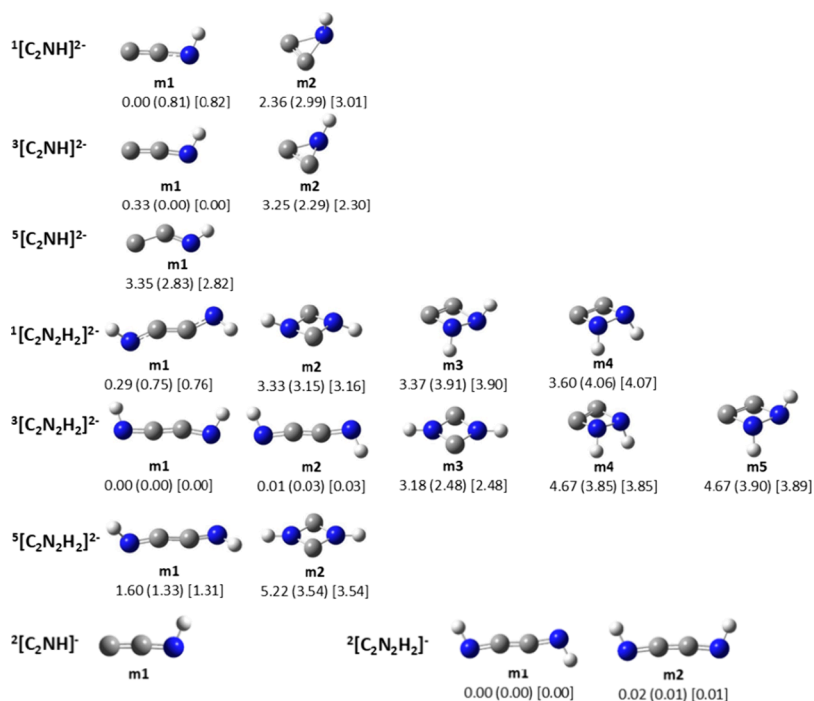


Figure 2. Minimum structures and relative energies in eV of the $[\text{C}_2\text{NH}]^{2-}$ and $[\text{HNC}_2\text{NH}]^{2-}$ anions at the B3LYP/6–311+G(d,p), (CCSD(T)/aug-cc-pVTZ), and [QCISD(T)/aug-cc-pVTZ] methods.

majority of the dianions in solid state or in solutions cannot exist as isolated species, while they decay in the gas phase by electron autodetachment.^{14,15} Evidence of the dianions has been obtained via mass spectroscopy.^{12,13} The $[\text{C}_2]^{2-}$ is the simplest dianion; it is a metastable system, and its lifetime has been measured at 0.1 fs.¹⁶ Its electronic structure has been calculated via perturbation theory and multireference interaction methodologies^{17–19} and its lifetime has been calculated at 2.5 fs.¹⁹

Given that the $[\text{C}_2]^{2-}$ dianion is metastable due to an autodetachment process, where an autoionization process occurs, and the electron is spontaneously emitted, a question arises. Can the attachment of one or two NH stabilize the

$[\text{C}_2]^{2-}$ dianion? In other words, can the dianions $[\text{C}=\text{C}-\text{NH}]^{2-}$ and $[\text{HN}-\text{C}=\text{C}-\text{NH}]^{2-}$ be experimentally observed?

Although the electronic structure and reactivity of nitrogen-centered radicals have been studied, the influence of NH attachment on N_3H and, particularly, its effect on chemical bonding have not been investigated. Furthermore, there is a gap in the literature regarding studies of $[\text{C}_2\text{N}_2\text{H}_2]$ specific moieties; note that they are integrated only as part of larger studies on nitrogen compounds or nitrogen fixation intermediates.¹¹ In addition, we are not aware of any theoretical or experimental reports on the possible formation of dianions $[\text{C}_2\text{NH}]^{2-}$ and $[\text{HNC}_2\text{NH}]^{2-}$. Thus, the present study seeks to fill this gap in the literature.

In the present paper, the chemical bonding, the molecular and electronic structures, and the dissociation energies of the N_3H and N_4H_2 molecules with respect to $HN + N_2$ molecules are studied. Furthermore, their isoelectronic $[C_2NH]^{2-}$ and $[C_2N_2H_2]^{2-}$ anions are calculated as well as those of the $[C_2NH]^-$ and $[C_2N_2H_2]^-$ anions. Their binding energies and thermochemical stability have been studied via density functional theory (DFT), coupled cluster (CC), configuration interaction (CI), and multireference configuration interaction (MRCI) methodologies. The present study aims to (1) study the effect of the NH attachment on N_3H and $[C_2NH]^{2-}$ regarding their chemical bonding and stability; (2) decipher the differences in electronic structure and chemical bonding between the isoelectronic N_3H and $[C_2NH]^{2-}$ or between the isoelectronic N_4H_2 and $[C_2N_2H_2]^{2-}$; (3) evaluate the effect of the NH bonding on the metastable $[C_2]^{2-}$ dianion; and (4) predict if the formed dianions $[C_2NH]^{2-}$ and $[C_2N_2H_2]^{2-}$ can remain for experimental observation. Finally, it should be noted that this study can be further expanded to other isoelectronic systems, such as those involving carbon–nitrogen or carbon–carbon species with similar bonding motifs, which could highlight broader principles governing stability and bonding differences. These directions would advance the chemical understanding of these isoelectronic moieties and related species, exploring potential applications in materials science or nitrogen chemistry.

2. COMPUTATIONAL DETAILS

First, a DFT conformation analysis of the N_3H and N_4H_2 molecules and of the isoelectronic $[C_2NH]^{2-}$ and $[C_2N_2H_2]^{2-}$ dianions were carried out for the singlet, triplet and quintet spin states, as well as for the $[C_2NH]^-$ and $[C_2N_2H_2]^-$ anions, at the B3LYP^{20,21}/6–311G+(d,p)²² level of theory, see Figures 1 and 2. For simplicity, the multiplicity of spin is given as a superscript in the molecular type, for example, 1N_3H or $^5[C_2N_2H_2]^{2-}$, see Figures 1 and 2. For all minima structures, their frequencies were calculated to confirm that they are true minimum structures. Furthermore, to check their stability, molecular dynamics simulations (MD)²³ for the lowest minima have been carried out via a classical trajectory calculation²⁴ using a Born–Oppenheimer molecular dynamics model²⁵ at the B3LYP/6–311G+(d,p) level of theory. The vibrational and rotational sampling temperature is 300 K, and a step size of 0.25 amu^{1/2}bohr was used for all calculations. MD calculations showed that the minimum structures remain stable. Note that the calculation of trajectories via the B3LYP/6–311+G(d,p) has been evaluated as adequate in small molecular systems such as the photodissociation of formaldehyde.²³

Then, for the lowest in energy minima structures and additional single point calculations were performed at the coupled cluster singles + doubles + perturbative triples [CCSD(T)]^{26,27} and quadratic configuration interaction + single + double + perturbative triples [QCISD(T)]^{28,29} employing the aug-cc-pVTZ basis set.³⁰ For the lowest-energy minimum structures, the geometries were optimized at the CCSD(T) level of theory. In some cases, the bond distances alter up to 0.03 Å; however, the energy differences between the single point CCSD(T)/B3LYP energies and optimized CCSD(T) energies range from 0.004 to 0.03 eV. Thus, the energetics have been calculated at the CCSD(T)/aug-cc-pVTZ level of theory, which is widely accepted as an adequate method for high-quality correlated calculations of small to medium molecules. Previous studies benchmark CCSD(T)/

aug-cc-pVTZ results for multiple reaction energies and find it sufficiently accurate to serve as a reference method against which lower-cost methods are compared.³¹

Furthermore, a complete active space self-consistent field (CASSCF) calculation was carried out by allotting the 16 “valence” electrons, namely, H(1s)¹ and N or C[–](2s2p),⁵ to 11 valence orbitals of the N_3H and C_2NH^{2-} species. Then, multireference configuration interaction + single + double excitations (MRCISD) and the MRCISD+Q,³² where +Q is the Davidson correction, were employed. The MRCISD spaces range from 4×10^8 to 2×10^9 configuration state functions (CSFs). By applying the internal contraction approximation (icMRCI),³³ the size of the CI spaces is reduced by at least an order of magnitude. Furthermore, potential energy curves (PEC) were plotted with respect to $HN + N_2$ (or $[C_2]^{2-}$) products. It should be noted that the MRCISD+Q/aug-cc-pVTZ method can provide accurate excitation energies for a diverse set molecule including multireference systems, validating its use for such calculations.³⁴

The thresholds used for all calculations are 10^{-8} for the change of the total energy, maximum displacement convergence criterion is <0.0012 Å. DFT, QCISD(T), CCSD(T), and DFT-MD calculations were carried out via Gaussian16,³⁵ CASSCF, icMRSISD(+Q), and CCSD(T) calculations were carried out via Molpro2022.3.³⁶

3. RESULTS AND DISCUSSION

First the diatomic N_2 , $[C_2]^{0,-,2-}$, and NH species were calculated at the B3LYP, CCSD, CCSD(T), QCISD(T), MRCISD, and MRCISD+Q/aug-cc-pVTZ methodologies, i.e., the same methodologies employed for the N_2NH , HNN_2NH , $[C_2NH]^{2-,-}$ and $[HNC_2NH]^{2-,-}$ moieties in order to validate our computational approach and to determine the binding energies. For the N_2 , $[C_2]^{2-}$, and NH, both their ground and excited states were calculated, see Table 1. The available experimental values, as well as the maximum and minimum deviation between the experimental data and the present calculations, as well as the average deviation of all calculated states of the six molecules or anions, are also included. It was found that all methodologies predict very well the geometries of the calculated states, i.e., they agree with available experimental results,^{37–40} and the average deviation is 0.001 Å, see Table 1. The corresponding energetics are also well predicted. The dissociation energies obtained via the CCSD(T), QCISD(T), and MRCISD+Q methodologies are in very good agreement with the available experimental values. Their absolute values of the deviation range from 0.02 to 0.74 eV for CCSD(T), 0.03 to 0.75 eV for QCISD(T), and 0.03 to 0.57 eV for MRCISD+Q. The largest deviation from the experimental values is obtained for the $a^3\Sigma_u^+$ state of N_2 . The difference between the calculated relative energies of the excited states for each molecule and the experimental energies is only up to 0.16 eV for the MRCISD+Q method, showing excellent agreement between theory and experiment. Below, the calculated data are reported in more detail along with published data.

Both N_2 and $[C_2]^{2-}$ form a triple bond $\sigma^2\pi^2\pi^2$ in their ground $X^1\Sigma_g^+$ state. The state is a single reference state; i.e., the MRCISD coefficient of their main configuration is about 0.95, showing that B3LYP, CCSD(T), and QCISD(T) are appropriate for its calculation. Note that while the X states of both molecules form triple bond, the dissociation energy (D_e) of the $[C_2]^{2-}$ is about 1/3 of the D_e value of the N_2 , i.e.,

Table 2. Bond Distances R (Å), Angles φ (Degrees) and Dipole Moments μ (D) of the Calculated Minimum Structures of the $^{1,3,5}\text{N}_2\text{NH}$, $^{1,3,5}[\text{C}_2\text{NH}]^{2-}$, and $^2[\text{C}_2\text{NH}]^-$ Species at the B3LYP/6-311+G(d,p) and RCCSD(T)/aug-cc-pVTZ^a Methods

molecule	structure	$R_{\text{X-X}}^b$	$R_{\text{X-NH}}$	$R_{\text{N-H}}$	φ_{HNX}	φ_{NXX}	μ	
$^1\text{N}_2\text{NH}$	m1	1.130	1.239	1.020	110.36	171.02	1.964	
	^a	1.136	1.249	1.019	108.48	171.31		
	m2	1.189	1.541	1.028	102.41	67.30	1.612	
$^3\text{N}_2\text{NH}$	m1	1.183	1.408	1.032	102.86	120.87	2.180	
	m2	1.464	1.363	1.026	123.33	57.54	2.713	
$^5\text{N}_2\text{NH}$	m1	1.479	1.259	1.036	120.92	113.47	2.088	
	m1	1.271	1.360	1.026	108.25	176.87	6.706	
$^1[\text{C}_2\text{NH}]^{2-}$	m2	1.329	1.650	1.030	104.47	66.27	4.256	
	$^3[\text{C}_2\text{NH}]^{2-}$	m1	1.285	1.286	1.031	111.55	173.06	2.363
		^a	1.295	1.299	1.024	112.88	173.06	
$^5[\text{C}_2\text{NH}]^{2-}$	m2	1.402	1.433	1.032	129.92	60.71	1.797	
	m1	1.460	1.252	1.036	117.00	134.15	1.924	
$^2[\text{C}_2\text{NH}]^-$	m1	1.282	1.298	1.026	109.94	175.45	4.436	

^aRCCSD(T)/aug-cc-pVTZ. ^bThe X atom corresponds to the N or C atom of the N_2 or $[\text{C}_2]^{2-}$.

3.12(3.19)[2.98] eV and 9.75(9.44)[9.42] eV at the B3LYP-(RCCSD(T)) [MRCISD+Q] methods; obviously the weakening of the D_e value of the triple bond of the $[\text{C}_2]^{2-}$ compared to N_2 is due to the double negative charge of the $[\text{C}_2]^{2-}$ species. The first excited state of both the N_2 and $[\text{C}_2]^{2-}$ species is the $a^3\Sigma_u^+$ state, where a double $\sigma^2\pi^2$ bond is formed. Again, the D_e value of $[\text{C}_2]^{2-}$ is smaller than the D_e value of the N_2 ; however, the D_e values differ only by about 0.9 eV, and thus the corresponding R_e values of the $a^3\Sigma_u^+$ state of the N_2 and $[\text{C}_2]^{2-}$ species differ only by about 0.01 Å. On the contrary, the R_e values of the ground states differ significantly by about 0.2 Å in accordance with the large value of the binding energy in N_2 . Finally, the relative energy (T_e) of the two states is about 6.50(6.15) eV for the N_2 molecule and 4.75(4.95) eV for the $[\text{C}_2]^{2-}$ anion by the RCCSD(T) (MRCISD+Q) methods. Experimentally, only the corresponding T_e value for the N_2 is available, namely $T_e = 6.223$ eV, in good agreement with our calculated values.

Among $[\text{C}_2]^{2-}$, $[\text{C}_2]^-$, and C_2 , $[\text{C}_2]^-$ is the lowest in energy species. The ground $X^2\Sigma_g^+$ state of the $[\text{C}_2]^-$ anion is a single reference state where two and a half bonds, $\sigma^1\pi^2\pi^2$, are formed. Both C species have 1.72 eV at the 2s orbital, and the bond is formed between $\text{C}(^3\text{P}) + \text{C}(^4\text{S})$, so the C atom is not excited in the ^5S state, which corresponds to the sp^3 hybridization. The $[\text{C}_2]^{2-}$ is the simplest dianion; it is a metastable system, and its lifetime has been measured at 0.1 fs.¹⁶ Here, it was found that the $X^1\Sigma_g^+$ state of the $[\text{C}_2]^{2-}$ is lying 3.62(3.63)[3.85] eV above the $X^2\Sigma_g^+$ state of $[\text{C}_2]^-$ at the B3LYP(CCSD(T))- [MRCISD+Q] methods in good agreement with the previously calculated value of 3.5 eV.¹⁹

Regarding the NH molecule, both the $X^3\Sigma^-$ and $a^1\Delta$ states have a σ^2 bond. Specifically, in the $X^3\Sigma^-$ state, the bond is formed from the atomic ground state of $\text{N}(^4\text{S})$, while in the $a^1\Delta$ state, the bond is formed from the atomic excited state $\text{N}(^2\text{D})$; the corresponding valence orbitals are $1\sigma^22\sigma^21\pi^11\pi^1$ ($X^3\Sigma^-$) and $1\sigma^22\sigma^21\pi^2$ ($a^1\Delta$). The D_e value of X state is 3.49(3.50) eV at RCCSD(T)[MRCISD+Q] methods in excellent agreement with available theoretical results⁴¹ and the experimental value of 3.47 eV.³⁷ Finally, the ground state of the NH^- anion, $X^2\Pi$, was calculated, which correlates to $\text{N}^- (^3\text{P}) + \text{N}(^2\text{S})$. It is more stable than the neutral atom by 0.23 eV at the RCCSD(T)/aug-cc-pVTZ. The dissociation energy

was calculated at 4.03 eV and the formed bonding is a σ^2 bond, see Table 1.

3.1. N_2NH and HNN_2NH

Many different structures of the N_2NH and HNN_2NH molecules of the singlet, triplet, and quintet spin states were investigated. The obtained minimum structures are shown in Figure 1, while selected geometries are given in Tables 2 and 3. For both molecules, the lowest energy N_2NH and HNN_2NH structures are singlet spin states. Their triplet states are 2.40 and 1.75 eV higher in energy, respectively, at RCCSD(T)/aug-cc-pVTZ, while the quintet states are 5.62 and 4.46 eV, respectively, see Figure 1. Finally, note that the N_2NH and HNN_2NH structures are open structures, the closed ring structures, i.e., structures having a triangular N_3 or square N_4 , are higher in energy by 1.65 and 0.58 eV, respectively.

The global minimum structure of the N_2NH (m1) is obtained via the formation of a dative bond between the $\text{N}_2(X^1\Sigma_g^+)$ and the $\text{NH}(a^1\Delta)$ molecules, i.e., $\text{N}\equiv\text{N}\rightarrow\text{N}-\text{H}$. Specifically, in the $\text{NH}(a^1\Delta)$ state, the $\text{N}(^2\text{D}; |2s^22p_0^12p_{+1}^2p_{-1}^0\rangle)$ forms a σ^2 bond with the $\text{H}(^2\text{S})$, while the empty $2p^0$ of the N of NH forms a dative bond with the $2s^2$ orbital of the N of N_2 , Scheme 1. As a result, both Mulliken and NBO analysis show that about 0.6 eV is transferred from $\text{N}\equiv\text{N}$ to the N atom of the $\text{NH}(a^1\Delta)$ molecule via the dative bond, while the N atom of the N_2 that forms this dative bond is positively charged, see Table 4 and Table 4S of Supporting Information (SI). The valence molecular orbitals related to chemical bonding (see Scheme 1) are shown in Figure S1 and SI. Regarding the geometry of the $^1\text{N}_2\text{NH}$ (m1), bond distances indicate the states involved in the diatomic molecules, i.e., $\text{N}_2(X^1\Sigma_g^+) + \text{NH}(a^1\Delta)$ molecules. The $\text{N}\equiv\text{N}$ distance is only by 0.03 Å elongated with respect to the free diatomic N_2 molecule, while the $\text{N}-\text{H}$ is shorter in the N_2NH (m1) by 0.02 Å than the diatomic $\text{NH}(a^1\Delta)$ molecule. The $^1\text{N}_2\text{NH}$ (m1) molecule has a planar geometry, and the angle φ_{HNX} is 110 degrees, close to 90 deg, since the dative bond is perpendicular to the σ^2 bond of the NH . Finally, the PEC of the N_2NH molecule with respect to the $\text{N}_2 + \text{NH}$ at all used multireference levels of theory is depicted in Figure 3, where clearly shown that the PEC correlates to $\text{N}_2(X^1\Sigma_g^+) + \text{NH}(a^1\Delta)$. The formation energies ΔE_r of the $\text{NH} + \text{N}_2 \rightarrow \text{N}_2\text{NH}$ at the CCSD(T)[QCISD(T)] {MRCISD+Q}/aug-cc-pVTZ is calculated at $-2.59[-2.61]\{2.32\}$ eV, see Figure 3 and Table

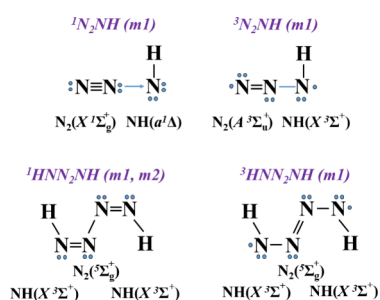
Table 3. Bond Distances R (Å), Angles φ (Degrees) and Dipole Moments μ (D) of the Calculated Minimum Structures of the $^{1,3,5}\text{HNN}_2\text{NH}$, $^{1,3,5}[\text{HNC}_2\text{NH}]^{2-}$ and $^2[\text{HNC}_2\text{NH}]^-$ Species at the B3LYP/6-311+G(d,p) and RCCSD(T)/aug-cc-pVTZ^a

Methods

str.	$R_{\text{X-X}}^b$	$R_{\text{X-NH}}$	$R_{\text{N-H}}$	$R_{\text{HN-NH}}$	φ_{HNX}	φ_{NXX}	d_{NXXN}	d_{HNNH}	μ
¹HNN₂NH									
m1	1.405	1.232	1.030		106.13	113.57	89.28		0.194
	1.439	1.242	1.028		105.40	110.21	88.03		
m2	1.559	1.214	1.044		111.15	111.64	180.00		0.000
	1.526	1.231	1.041		109.59	111.01	180.00		
m3	1.277	1.401	1.022	1.443	114.28	93.01	9.61	121.52	3.065
m4	1.277	1.402	1.020	1.438	115.06	93.29	0.00	0.00	4.075
m5	2.022	1.357	1.013	1.356	126.64	83.63	-0.09		0.021
³HNN₂NH									
m1	1.286	1.269	1.023		106.93	123.24	180.00		0.000
	1.293	1.276	1.023		105.91	122.27	180.00		
m2	1.239	1.285	1.024		108.62	126.49	0.00		0.967
m3	1.988	1.432	1.023	1.431	112.73	86.13	25.62		1.531
m4	2.019	1.431	1.026	1.431	113.00	88.02	-15.83		1.069
m5	1.427	1.412, 1.481	1.026	1.445	115.46	85.20	-19.74	153.92	2.267
	1.448	1.390, 1.455	1.029	1.461	116.15	85.58	22.14	8.44	3.848
⁵HNN₂NH									
m1	1.382	1.313	1.034		111.54	115.76	77.38		0.769
m2	1.382	1.303	1.033		113.09	117.32	109.36		3.157
m3	1.381	1.308	1.033		111.76	116.87	92.75		2.221
m4	1.422	1.291, 1.364	1.032	1.022	113.59	116.34	62.62		1.359
¹[HNC₂NH]²⁻									
m1	1.286	1.348	1.017		108.55	150.16	114.64		0.456
m2	2.155	1.442	1.015		125.42	83.28	0.00		0.006
m3	1.381	1.535	1.030	1.494	108.83, 108.86	91.89, 87.72	6.59	135.92	7.776
m4	1.377	1.540	1.030	1.511	107.38, 107.37	92.48, 87.51	-0.02	0.00	8.045
³[HNC₂NH]²⁻									
m1	1.254	1.303	1.027		110.35, 108.59	167.13, 175.79	179.93		5.586
m2	1.252	1.311	1.028		109.29	171.96	180.00		0.000
	1.264	1.317	1.024		109.90	166.77	180.00		
m3	2.109	1.423	1.006		132.16	84.36	-0.04		0.003
m4	1.366	1.428, 1.567	1.037	1.506	112.15, 108.93	102.14, 90.06	10.66	10.75	3.679
	1.345	1.631, 1.418	1.030	1.513	104.61, 111.48	81.16, 106.13	4.50	140.98	5.592
⁵[HNC₂NH]²⁻									
m1	1.284	1.245	1.030		121.31	168.21	114.21		1.898
m2	1.949	1.388	1.016		135.44	90.84	0.00		0.003
²[HNC₂NH]⁻									
m1	1.252	1.309	1.024	3.861	109.77	171.34	180.00	180.00	0
m2	1.251	1.309	1.024	3.858	109.99	174.53	0.08	0.000	3.040

^aRCCSD(T)/aug-cc-pVTZ. ^bThe X atom corresponds to the N or C atom of the N₂ or [C₂]²⁻.

Scheme 1. Chemical Bonding of the $^{1,3}\text{N}_2\text{NH}$ and $^{1,3}\text{HNN}_2\text{NH}$ Molecules



5. Our best value is obtained with the CCSD(T) and QCISD(T) methods. Note that the coefficient of the main configuration function of the CASSCF(MRCISD) method is

0.95(0.91), and thus, the state can be considered as a mainly single-reference state. Finally, it should be noted that the $^1\text{N}_2\text{NH}$ (m1) molecule is lower in energy than the ground state of the diatomic molecules by 0.69[0.71] eV.

The lowest in energy triplet state, i.e., $^3\text{N}_2\text{NH}$ (m1), is formed via the $\text{N}_2(A^3\Sigma_u^+) + \text{NH}(X^3\Sigma^-)$ via the formation of a covalent bond, see Scheme 1, which is formed between two p¹ orbitals of the adjacent N atoms, and as a result, the φ_{NXX} angle is 102.9 degrees, see Table 2. While the two unpaired electrons are originally located at the two remote N atoms, they are delocalized in the whole molecule, as is shown from the valence molecular orbitals in Figure S1 of SI and Tables S5–S6. The PEC of the $^3\text{N}_2\text{NH}$ molecule with respect to the N₂ + NH shows an avoided crossing at about 1.8 Å between two states correlated to $\text{N}_2(A^3\Sigma_u^+) + \text{NH}(X^3\Sigma^-)$ and $\text{N}_2(X^1\Sigma_g^+) + \text{NH}(X^3\Sigma^-)$, see Figure 3. The reaction energies with respect to the in situ diatomic molecules, i.e., $^3\text{N}_2\text{NH}$ (m1) \rightarrow $\text{N}_2(A^3\Sigma_u^+) +$

Table 4. Mulliken and NPA Charges of the Atoms of the Selected Minimum Structures of the $^{1,3,5}\text{N}_2\text{NH}$, $^{1,3,5}\text{HNN}_2\text{NH}$, $^{1,3,5}[\text{C}_2\text{NH}]^{2-}$, $^{1,3,5}[\text{HNC}_2\text{NH}]^{2-}$, $^2[\text{C}_2\text{NH}]^-$, and $^2[\text{HNC}_2\text{NH}]^-$ Species in the B3LYP/6-311+G(d,p) Method

species	minimum	population Analysis	H	N	X	X	N	H
$^1\text{N}_2\text{NH}$	m1	Mulliken			-0.05	0.50	-0.69	0.25
		NPA			-0.06	0.22	-0.53	0.37
$^3\text{N}_2\text{NH}$	m1	Mulliken			-0.08	0.01	-0.16	0.23
		NPA			0.02	-0.10	-0.23	0.31
$^1\text{HNN}_2\text{NH}$	m1	Mulliken	0.26	-0.40	0.14	0.14	-0.40	0.26
		NPA	0.33	-0.31	-0.01	-0.01	-0.31	0.33
$^3\text{HNN}_2\text{NH}$	m1	Mulliken	0.27	-0.32	0.05	0.05	-0.32	0.27
		NPA	0.34	-0.35	0.01	0.01	-0.35	0.34
$^1[\text{C}_2\text{NH}]^{2-}$		NPA			-1.02	-0.10	-1.16	0.27
$^3[\text{C}_2\text{NH}]^{2-}$	m1	NPA			-0.64	-0.53	-1.05	0.21
$^1[\text{HNC}_2\text{NH}]^{2-}$	m1	NPA	0.28	-1.05	-0.23	-0.23	-1.05	0.28
$^3[\text{HNC}_2\text{NH}]^{2-}$	m1	NPA	0.27	-0.92	-0.10	-0.46	-1.01	0.22
$^3[\text{HNC}_2\text{NH}]^{2-}$	m2	NPA	0.25	-0.98	-0.27	-0.27	-0.98	0.25
$^2[\text{C}_2\text{NH}]^-$	m1	Mulliken			-0.47	-0.08	-0.74	0.30
		NPA			-0.59	-0.05	-0.53	0.16
$^2[\text{HNC}_2\text{NH}]^-$	m1	Mulliken	0.15	-0.59	-0.06	-0.06	-0.59	0.15
		NPA	0.30	-0.83	0.04	0.04	-0.83	0.30
$^3[\text{HNC}_2\text{NH}]^-$	m2	Mulliken	0.15	-0.62	-0.03	-0.03	-0.62	0.15
		NPA	0.30	-0.83	0.04	0.04	-0.83	0.30

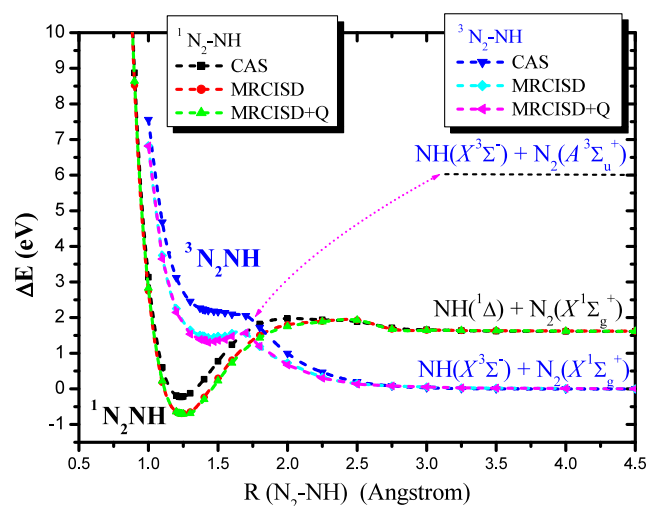


Figure 3. Potential energy curves of the dissociation of the $\text{N}_3\text{H} \rightarrow \text{N}_2 + \text{NH}$ at the CASSCF, MRCISD, and MRCISD+Q/aug-cc-pVTZ levels of theory. As zero energy has been assigned the diatomic ground state products.

+ $\text{NH}(X^3\Sigma^-)$ is $-4.99[-4.72]$ eV at the CCSD(T)[MRCISD+Q]/aug-cc-pVTZ method, however with respect to the correlated diatomic products, i.e., $\text{N}_2(X^1\Sigma_g^+) + \text{NH}(X^3\Sigma^-)$, is 1.71 eV, see Table 5 and Figure 3. Note that the minimum $^3\text{N}_2\text{NH}$ (m1) is very shallow, even though it is a true minimum. However, it breaks very easily, and a linear van der Waals dimer $\text{N}-\text{H}\cdots\text{N}\equiv\text{N}$ is formed with a $\text{H}\cdots\text{N}$ bond distance of 2.600 Å and a formation energy of -0.03 eV, at the RCCSD(T)/aug-cc-pVTZ level of theory. Similarly to the previous singlet state structure, the coefficient of the main configuration function of the CASSCF(MRCISD) method is 0.95(0.91), and thus, the state can also be considered as a mainly single-reference state.

The addition of a second NH at the N_2NH molecule results in the HNN_2NH molecule, see Figure 1, however this addition affects the bonding of the N_2 central group. If the bonding of

the N_2NH was retained in the HNN_2NH molecule, it would be expected that the bonding would be $\text{H}-\text{N}\leftarrow\text{N}\equiv\text{N}\rightarrow\text{N}-\text{H}$; however, calculations show that this does not occur in the lowest energy state, and the molecule presents a different bonding scheme.

Thus, for the $^1\text{HNN}_2\text{NH}$ molecule, two minima, m1 and m2, are calculated as the lowest ones, see Figure 1. They present some differences in their geometry; however, they are energetically degenerate; see Figure 1. In both minima, the triple bond of the N_2 becomes single, and its N atoms form double bonds with the $\text{NH}(X^3\Sigma^-)$. For both m1 and m2 structures, the *in situ* diatomic molecules are $\text{NH}(X^3\Sigma^-) + \text{N}_2(^5\Sigma_g^+) + \text{NH}(X^3\Sigma^-)$. The m1 and m2 differ in which p electrons of the N atoms of the N_2 formed the single bond in N_2 , and which p electrons formed a double bond with the NH molecules. Thus, in m1 the two $\text{HN}=\text{N}$ atoms are perpendicular to each other, while in m2 they belong to the same plane; see Figure 1. Furthermore, since the p electrons of the N atoms are involved in the bonding, the φ_{HNX} and φ_{NXX} angles are about 110 degrees. The fact that there are about 110 degrees and not ~ 90 deg is due to the steric effect. If the N-H and N-N distances were larger, it would be expected to have HNN angles of 90 deg.⁴² Moreover, only the N atoms of NH are negatively charged by about 0.4 e^- , while the central N atoms are not charged. The $^1\text{HNN}_2\text{NH}$ (m1 and m2) are stable and the reaction energy with respect to the ground state diatomic molecules, i.e., $\text{N}_2(X^1\Sigma_g^+) + 2 \times \text{NH}(X^3\Sigma^-)$ is about -2.8 eV at both RCCSD(T) and QCISD(T) levels of theory, while with respect to the *in situ* diatomic products, i.e., $2 \times \text{NH}(X^3\Sigma^-) + \text{N}_2(^5\Sigma_g^+)$, is -11.93 eV.

The lowest in energy triplet state, i.e., $^3\text{HNN}_2\text{NH}$ (m1), is formed via the $\text{NH}(X^3\Sigma^-) + \text{N}_2(a^3\Sigma_u^+) + \text{NH}(X^3\Sigma^-)$ via the formation of a single covalent bond of N_2 with each NH, see Scheme 1. The geometry of the $\text{N}_2(a^3\Sigma_u^+)$ is retained in the $^3\text{HNN}_2\text{NH}$ (m1), the R_e distance of the $\text{N}=\text{N}$ is elongated only 0.008 Å, cf. Table 1 and Table 3. While the two unpaired electrons are originally located at the two remote N atoms of NH, they are delocalized in the whole molecule, as shown from

Table 5. Reaction Energies ΔE_r (eV), Reaction Enthalpies ΔH_r (eV) and Gibbs Free Energies ΔG_r (eV) of the $\text{NH} + \text{N}_2 \rightarrow \text{N}_2\text{NH}$ and $2 \times \text{NH} + \text{N}_2 \rightarrow \text{HNN}_2\text{NH}$ Reactions at B3LYP/6–311+G(d,p), CCSD(T), QCISD(T), MRCISD, MRCISD+Q/aug-cc-pVTZ Levels of Theory

molecule ^a	reactants ^a	B3LYP			CCSD(T)	QCISD(T)	MRCISD(+Q) ^b
		ΔE_r	ΔH_r	ΔG_r	ΔE_r	ΔE_r	ΔE_r
¹ N ₂ NH (m1)	¹ N ₂ + ¹ NH	−3.14	−2.98	−2.60	−2.59(−2.59) ^c	−2.61	−2.30(−2.32)
¹ N ₂ NH (m2)	¹ N ₂ + ¹ NH	−1.17	−1.03	−0.66	−0.94	−0.95	
³ N ₂ NH (m1)	¹ N ₂ + ³ NH	1.30	1.37	1.71	1.71	1.68	1.58(1.35)
	³ N ₂ + ³ NH	−5.77	−5.66	−5.29	−4.99	−4.84	−4.56(−4.71)
³ N ₂ NH (m2)	¹ N ₂ + ³ NH	2.67	2.78	3.15	3.01	3.00	
N≡N...HN(X ³ Σ [−])					(−0.03) ^c		
⁵ N ₂ NH	³ N ₂ + ³ NH	−2.70	−2.62	−2.24	−2.40	−2.40	
¹ HNN ₂ NH (m1)	¹ NH + ¹ N ₂ + ¹ NH	−7.32	−6.97	−6.15	−6.58(−6.61) ^c	−6.59	
	³ NH + ¹ N ₂ + ³ NH	−2.95	−2.60	−1.72	−2.79(−2.82) ^c	−2.80	
¹ HNN ₂ NH (m2)	¹ NH + ¹ N ₂ + ¹ NH	−7.31	−6.99	−6.18	−6.60(−6.62) ^c	−6.62	
	³ NH + ¹ N ₂ + ³ NH	−2.94	−2.62	−1.75	−2.81(−2.83) ^c	−2.83	
¹ HNN ₂ NH (m3)	¹ NH + ¹ N ₂ + ¹ NH	−6.69	−6.31	−5.46	−6.03	−6.04	
	³ NH + ¹ N ₂ + ³ NH	−2.32	−1.94	−1.03	−2.24	−2.25	
³ HNN ₂ NH (m1)	¹ NH + ¹ N ₂ + ³ NH	−3.97	−3.67	−2.83	−2.96(−2.96) ^c	−3.01	
	³ NH + ³ N ₂ + ³ NH	−13.22	−12.89	−12.05	−11.55(−11.55) ^c	−11.42	
³ HNN ₂ NH (m2)	¹ NH + ¹ N ₂ + ³ NH	−3.69	−3.40	−2.60	−2.69	−2.73	
³ HNN ₂ NH (m3)	¹ NH + ¹ N ₂ + ³ NH	−2.17	−1.85	−1.00	−1.59	−1.61	
⁵ HNN ₂ NH	³ NH + ¹ N ₂ + ³ NH	0.94	1.15	1.97	1.65	1.62	

^aMultiplicity of spin is provided as superscript at the left of each compound. ^bMRCISD (MRCISD+Q). ^cAt the optimized RCCSD(T)/aug-cc-pVTZ geometry.

the valence molecular orbitals in Figure S1 of SI and Tables S4–S5. The reaction energy with respect to the in situ diatomic molecules, i.e., $\text{NH}(X^3\Sigma^-) + \text{N}_2(A^3\Sigma_u^+) + \text{NH}(X^3\Sigma^-) \rightarrow {}^3\text{HNN}_2\text{NH}$ (m1) is −11.5 eV at the CCSD(T)/aug-cc-pVTZ method, however with respect to the correlated diatomic products, i.e., $\text{NH}(a^1\Delta) + \text{N}_2(X^1\Sigma_g^+) + \text{NH}(X^3\Sigma^-)$, is 3.0 eV at both CCSD(T) and QCISD(T) methods, see Table 5.

Finally, MD simulations were carried out for the lowest in energy minima m1 structures of the singlet states of the N_2NH and HNN_2NH molecules via a classical trajectory calculation using a Born–Oppenheimer molecular dynamics model at the B3LYP/6–311G+(d,p) level of theory. Starting from these minima structures, the molecules retained their structure during the MD simulations, meaning that both are stable. Additional MD calculations were carried out, where the $\text{N}_2\cdots\text{NH}$ and $\text{HNN}_2\cdots\text{NH}$ distances have been elongated at 2.0 Å, while the bond distances of the m1 structures are 1.225 Å (N_2NH) and 1.244 Å (HNN_2NH). After 33.8 and 14.9 fs, the m1 calculated minima structures were obtained, respectively.

3.2. $[\text{C}_2\text{NH}]^{2-}$ and $[\text{HNC}_2\text{NH}]^{2-}$

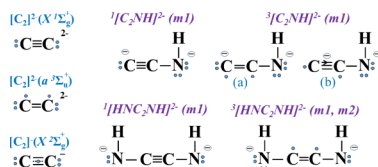
Different structures of the singlet, triplet, and quintet spin states of the $[\text{C}_2\text{NH}]^{2-}$ and $[\text{HNC}_2\text{NH}]^{2-}$ dianions were investigated, see Figure 2, while selected geometries are given in Tables 2 and 3. Regarding the $[\text{C}_2\text{NH}]^{2-}$ dianion, all methodologies apart from DFT/B3LYP, predict a triplet state as the ground state. B3LYP predicts a singlet one as the lowest in energy structure, but the energy difference between the singlet and triplet state is only 0.33 eV. Multireference methods also predict the triplet one as the lowest in energy; however, the singlet and triplet state is almost energetically degenerated. Regarding the $[\text{HNC}_2\text{NH}]^{2-}$ dianion, all methodologies, including the DFT, predict the triplet state as the ground state. At the CCSD(T)/aug-cc-pVTZ method, the

lowest in energy singlet structures are 0.81 and 0.75 eV higher in energy than the triplet ones for the $[\text{C}_2\text{NH}]^{2-}$ and $[\text{HNC}_2\text{NH}]^{2-}$, respectively. The quintet states are 2.83 and 1.33 eV, respectively, see Figure 2. Finally, as in the cases of the N_2NH and HNN_2NH molecules, where the lowest minimum structures are open structures, while the closed ring structures, i.e., structures having a triangular N_3 and tetragonal N_4 are higher in energy, similarly the $[\text{C}_2\text{NH}]^{2-}$ and $[\text{HNC}_2\text{NH}]^{2-}$ dianions are open structures and the closed ring structures, i.e., structures having a triangular C_2N and tetragonal C_2N_2 are higher in energy, by 2.29 and 2.48 eV, respectively. Regarding the geometries, the C–C bond distances range from 1.27 to 1.46 Å, and the corresponding formed bonds range from a single bond (quintet states) to a triple one (singlet states); see Tables 2 and 3 and discussion below. Finally, when there is no direct bond between the two C atoms, their distances are observed at ~2.1 Å; see Table 3 and Figure 2.

Both global minimum structures of triplet and singlet multiplicity of spin ${}^3[\text{C}_2\text{NH}]^{2-}$ (m1) and ${}^1[\text{C}_2\text{NH}]^{2-}$ (m1) are stable with respect to $[\text{C}_2]^{2-}(X^1\Sigma_g^+) + \text{NH}(X^3\Sigma^-)$ and $[\text{C}_2]^{2-}(X^2\Sigma_g^+) + [\text{NH}]^{2-}(X^2\Pi)$ products. It is interesting to find out if their bonding is the same as that of the isoelectronic N_2NH species, or if the stable $[\text{C}_2]^-$ is involved. Note that $[\text{C}_2]^-$ is more stable than $[\text{C}_2]^{2-}$ by 3.62 eV, and $\text{NH}^{2-}(X^2\Pi)$ is more stable than NH by 0.23 eV at the CCSD(T)/aug-cc-pVTZ, thus the electron transfer is favored by both diatomic parts. It should be noted, while in the case of the N_2NH species both population analyses, Mulliken and NPA, predict similar atomic electron charges, for the $[\text{C}_2\text{NH}]^{2-}$ dianion, Mulliken charges are not reasonable, i.e., very large electron charges are observed in some cases, more than 2 e[−] are transferred among atoms, and thus they have not been considered. Regarding the NPA analysis, see Table S5 and SI, in the equilibrium of the ${}^3[\text{C}_2\text{NH}]^{2-}$ (m1) structure and ${}^1[\text{C}_2\text{NH}]^{2-}$ (m1) structure, one electron is transferred from

$[\text{C}_2]^{2-}$ to the NH, as it is shown via the atomic population analysis, see Table 4. In the singlet state, the electron charge of the $[\text{C}_2]^-$ anion is in the remote C atom, while in the triplet state, the charge is distributed in both C species, with the remote C atom having the largest charge. Furthermore, in both singlet and triplet states, NPA shows that the natural electron configuration of the C atom, which forms a bond with N, is about $2s^{0.92}2p^{3.13}$, see Table S5 of SI, showing that this C species is in its ^5S state. In the singlet state, a triple bond in form in the $[\text{C}_2]^-$ and a covalent bond between the C atom and the N^- , see Scheme 2. Due to this bonding, the φ_{NXX} angle

Scheme 2. Chemical Bonding of the $^1,^3[\text{C}_2\text{NH}]^{2-}$ and $^1,^3[\text{HNC}_2\text{NH}]^{2-}$ Dianions



is 177 degrees, see Table 2, i.e., the $\text{C}\equiv\text{C}-\text{N}$ group is almost linear. In the triplet state, the bonding is depicted in Scheme 2, where two configurations, (a) and (b), have been considered. In the (a) configuration, the bond in the $[\text{C}_2]^-$ part is a double covalent bond. In the (b) configuration, an additional bond has been considered where the $2s^2$ of the remote C atom with the $2s^1$ of the central C atom forms a bond of three electrons ($2s^22s^1$), two-center C–C. Both population analysis and molecular orbitals do not clearly show which one is the most possible configuration, and thus, both are reported. However, regardless of which configuration is the most possible one, it is clearly observed that the involved $[\text{C}_2]^-$ anion is in an excited state. Note that in the free $[\text{C}_2]^-$ ($X^2\Sigma_g^+$) anion, its bond is formed between $\text{C}(2s^22p^2)$ and $\text{C}^-(2s^22p^3)$, while in both $^3[\text{C}_2\text{NH}]^{2-}$ (m1) and $^1[\text{C}_2\text{NH}]^{2-}$ (m1) structures the central C atom is in its $^5\text{S}(2s^12p^3)$ state.

To further clarify the bonding PEC of both $^3[\text{C}_2\text{NH}]^{2-}$ and $^1[\text{C}_2\text{NH}]^{2-}$ states, the PEC of the states was plotted as the $\text{C}_2\cdots\text{NH}$ distance is increased, see Figure 4. Note that the triplet state is a single reference state; i.e., the CASSCF-(MRCISD) coefficient of the main configuration state is 0.95(0.90), while the singlet state is a multireference state,

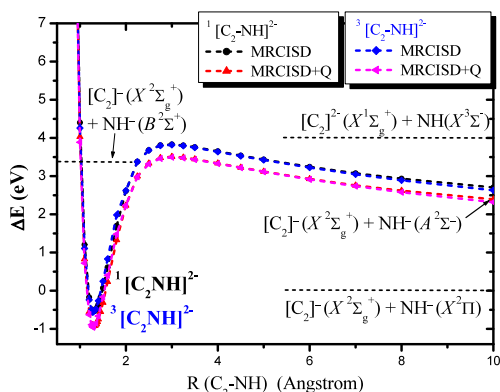


Figure 4. Potential energy curves of the dissociation of the $[\text{C}_2\text{NH}]^{2-} \rightarrow [\text{C}_2]^{2-n} + [\text{NH}]^n$, where $n = 0$ and 1 at the MRCISD, MRCISD+Q/aug-cc-pVTZ levels of theory. As zero energy has been assigned, the lowest diatomic products are $[\text{C}_2]^- (X^2\Sigma_g^+) + [\text{NH}]^- (X^2\Pi)$.

where in the equilibrium an open singlet configuration state function is involved with a CASSCF(MRCISD) coefficient of 0.88(0.84), while two closed shell singlet configuration states function with a coefficient of 0.25(0.24) each one. As mentioned before, in the equilibrium, the C atom in the middle is in its $^5\text{S}(2s^12p^3)$ state, and this state changes to the $^3\text{P}(2s^22p^2)$ state due to an avoided crossing around 2.8 Å. Thus, both states correlate to $[\text{C}_2]^- (X^2\Sigma_g^+) + \text{NH}^- (A^2\Sigma^-)$, see Figure 4. Note that the two states are almost energetically degenerate at the MRCISD level of theory, with the triplet one being the lowest one.

The reaction energies of different minima structures and different spin states with respect to possible $\text{NH}^+ + [\text{C}_2]^{2-n}$, $n = 0$, and -1 are given in Table 6. The reaction energy of the lowest triplet state with respect to the lowest ground state species is $[\text{C}_2]^- (X^2\Sigma_g^+) + \text{NH}^- (X^2\Pi) \rightarrow ^3[\text{C}_2\text{NH}]^{2-}$ (m1) is $-1.14\{-1.13\}[-0.97]$ eV at the CCSD(T){QCISD(T)}-[MRCISD+Q] methods, while for the reaction is $[\text{C}_2]^{2-} (X^1\Sigma_g^+) + \text{NH}(X^3\Sigma^-) \rightarrow ^3[\text{C}_2\text{NH}]^{2-}$ (m1) is $-4.99\{-5.00\}[-4.98]$ eV. Thus, all used methods result in the same reaction energies. Regarding the lowest singlet state, the calculated reaction energy with respect to the lowest ground state species is $[\text{C}_2]^- (X^2\Sigma_g^+) + \text{NH}^- (X^2\Pi) \rightarrow ^1[\text{C}_2\text{NH}]^{2-}$ (m1) is $-0.33\{-0.31\}[-0.94]$ eV at CCSD(T){QCISD(T)}-[MRCISD+Q], while for the reaction is $[\text{C}_2]^{2-} (X^3\Sigma_u^+) + \text{NH}(X^3\Sigma^-) \rightarrow ^1[\text{C}_2\text{NH}]^{2-}$ (m1) is $-5.31\{-5.30\}[-5.91]$ eV.

The addition of a second NH at the $[\text{C}_2\text{NH}]^{2-}$ molecule results in the $[\text{HNC}_2\text{NH}]^{2-}$ molecule, see Figure 2. This addition affects the bonding of the C_2 central group. In the equilibrium of the $^1[\text{HNC}_2\text{NH}]^{2-}$ (m1) molecule, the NPA shows that the electron configuration of both C atoms is $2s^{0.90}2p^{3.14}$, while adding in the $2s$ population, the electron charges of $3s$ and $4s$ orbitals become $2s^{1.05}2p^{3.18}$, showing that both C atoms are in their ^5S atomic state. The electron charge is transferred to the N atoms, and thus two NH^- anions are involved, while the C atoms are charged only by $-0.2 e^-$, see Table 4 and Table S5 of SI. The bonding is plotted in Scheme 2. The $\text{H}(1s^1)$ is bonded to the p^1 orbital of the N^- (^3P), while the other unpaired p^1 electron forms a bond with the $-\text{C}\equiv\text{C}-$, resulting in a CNH angle of about 111° , larger than the 90° due to the short N–H bond distance. The reaction energies resulting from the in situ diatomic species $\text{C}_2(X^1\Sigma_g^+) + 2 \times \text{NH}^- (X^2\Pi) \rightarrow ^1[\text{HNC}_2\text{NH}]^{2-}$ (m1) is $-7.82[-7.78]$ eV at the CCSD(T)[QCISD(T)] methodologies, with respect to the $[\text{C}_2]^{2-} (X^1\Sigma_g^+) + 2 \times \text{NH}(X^3\Sigma^-) \rightarrow ^1[\text{HNC}_2\text{NH}]^{2-}$ (m1) is $-8.74[-8.73]$ eV, while for the reaction with respect to the lowest in energy diatomic products $[\text{C}_2]^- (X^2\Sigma_g^+) + \text{NH}(X^3\Sigma^-) + \text{NH}^- (X^2\Pi) \rightarrow ^1[\text{HNC}_2\text{NH}]^{2-}$ (m1) is $-4.86[-4.85]$ eV.

For the $^3[\text{HNC}_2\text{NH}]^{2-}$ molecule, the two calculated minima, m1 and m2, are energetically degenerated, while there are differences in their geometry mainly regarding the relative position of the two H atoms, see Figure 2. Again, the electron charge is transferred to the N atoms, so the NH^- anions are involved in both $^3[\text{HNC}_2\text{NH}]^{2-}$ (m1) and (m2). The electron distribution of each C atom is about $2s^{0.83}2p^{3.10}$ at m1 and m2, see Table S5 of SI; meaning that two $\text{C}(^5\text{S})$ atomic states are involved. The bonding between the C atoms is a double bond, while one unpaired electron at each C atom exists, which presents a small interaction with the $3s$ unoccupied orbital of the other C atoms. This is the reason why the C atoms present about $3s^{0.25}$, while in the $^1[\text{HNC}_2\text{NH}]^{2-}$ (m1) molecule, the C atoms have $3s^{0.14}$. The

Table 6. Formation Energies ΔE_r (eV), Reaction Enthalpies ΔH_r (eV) and Gibbs Free Energies ΔG_r (eV) of the $\text{NH} + [\text{C}_2]^{2-} \rightarrow [\text{C}_2\text{NH}]^{2-}$ and $2 \times \text{NH} + [\text{C}_2]^{2-} \rightarrow [\text{HNC}_2\text{NH}]^{2-}$ Reactions at B3LYP/6-311+G(d,p), CCSD(T)/aug-cc-pVTZ and QCISD(T)/aug-cc-pVTZ Levels of Theory

molecule ^a	reactants ^a	B3LYP			CCSD(T)	QCISD(T)	MRCISD(+Q) ^b
		ΔE_r	ΔH_r	ΔG_r	ΔE_r	ΔE_r	ΔE_r
$^1[\text{C}_2\text{NH}]^{2-}$ (m1)	$^1[\text{C}_2]^{2-} + ^1\text{NH}$	-6.46	-6.33	-5.96	-6.08(-6.08) ^a	-6.07	-6.30(-6.61)
	$^3[\text{C}_2]^{2-} + ^3\text{NH}$	-6.56	-6.43	-6.00	-5.31(-5.31) ^a	-5.30	-5.43(-5.91)
	$^2[\text{C}_2]^- + ^2\text{NH}^-$	-0.25	-0.12	0.29	-0.33(-0.33) ^a	-0.31	-0.54(-0.94)
$^1[\text{C}_2\text{NH}]^{2-}$ (m2)	$^1[\text{C}_2]^{2-} + ^1\text{NH}$	-4.10	-4.00	-3.65	-3.90	-3.89	
	$^3[\text{C}_2]^{2-} + ^3\text{NH}$	-4.19	-4.10	-3.69	-3.13	-3.11	
$^3[\text{C}_2\text{NH}]^{2-}$ (m1)	$^1[\text{C}_2]^{2-} + ^3\text{NH}$	-3.95	-3.80	-3.42	-4.99(-4.99) ^a	-5.00	-4.64(-4.98)
	$^3[\text{C}_2]^{2-} + ^3\text{NH}$	-6.23	-5.68	-6.09	-6.12(-6.12) ^a	-6.12	-5.46(-5.94)
	$^3[\text{C}_2]^{2-} + ^1\text{NH}$	-8.41	-8.27	-7.89	-8.01(-8.01) ^a	-8.02	-7.14(-7.61)
	$^2[\text{C}_2]^- + ^2\text{NH}^-$	0.07	0.61	0.22	-1.14(-1.14) ^a	-1.13	-0.56(-0.97)
$^3[\text{C}_2\text{NH}]^{2-}$ (m2)	$^1[\text{C}_2]^{2-} + ^3\text{NH}$	-1.02	-0.92	-0.56	-2.71	-2.71	
	$^3[\text{C}_2]^{2-} + ^1\text{NH}$	-5.49	-5.39	-5.03	-5.73	-5.72	
$^5[\text{C}_2\text{NH}]^{2-}$	$^3[\text{C}_2]^{2-} + ^3\text{NH}$	-3.21	-3.11	-2.73	-3.29	-3.30	
$^1[\text{HNC}_2\text{NH}]^{2-}$ (m1)	$^1\text{NH} + ^1[\text{C}_2]^{2-} + ^1\text{NH}$	-12.70	-12.41	-11.61	-12.50(-12.53) ^a	-12.52	
	$^3\text{NH} + ^1[\text{C}_2]^{2-} + ^3\text{NH}$	-8.33	-8.04	-7.18	-8.71(-8.74) ^a	-8.73	
	$^3\text{NH} + ^3[\text{C}_2]^{2-} + ^1\text{NH}$	-12.79	-12.51	-11.65	-11.73(-11.76) ^a	-11.74	
	$^2\text{NH}^- + ^1[\text{C}_2] + ^2\text{NH}^-$	-8.27	-7.97	-7.14	-7.82	-7.78	
	$^2\text{NH}^- + ^2[\text{C}_2]^- + ^3\text{NH}$	-4.30	-4.01	-3.15	-4.86	-4.85	
$^1[\text{HNC}_2\text{NH}]^{2-}$ (m2)	$^1\text{NH} + ^1[\text{C}_2]^{2-} + ^1\text{NH}$	-9.65	-9.34	-8.51	-10.11(-10.13) ^a	-10.11	
	$^3\text{NH} + ^1[\text{C}_2]^{2-} + ^3\text{NH}$	-5.28	-4.97	-4.08	-6.32(-6.34) ^a	-6.32	
	$^3\text{NH} + ^3[\text{C}_2]^{2-} + ^1\text{NH}$	-9.74	-9.43	-8.55	-9.34(-9.36) ^a	-9.34	
$^3[\text{HNC}_2\text{NH}]^{2-}$ (m1)	$^1\text{NH} + ^1[\text{C}_2]^{2-} + ^3\text{NH}$	-10.80	-10.49	-9.69	-11.36	-11.38	
	$^3\text{NH} + ^1[\text{C}_2]^{2-} + ^3\text{NH}$	-8.62	-8.30	-7.47	-9.47	-9.48	
	$^1\text{NH} + ^3[\text{C}_2]^{2-} + ^1\text{NH}$	-15.26	-14.96	-14.16	-14.38	-14.39	
	$^3\text{NH} + ^3[\text{C}_2]^{2-} + ^3\text{NH}$	-10.89	-10.59	-9.73	-10.59	-10.60	
	$^2\text{NH}^- + ^2[\text{C}_2]^- + ^3\text{NH}$	-4.59	-4.28	-3.44	-5.61	-5.61	
	$^2\text{NH}^- + ^1[\text{C}_2] + ^2\text{NH}^-$	-8.56	-8.24	-7.43	-8.57	-8.53	
	$^3[\text{C}_2\text{NH}]^{2-} + ^3\text{NH}$	-4.67	-4.50	-4.05	-4.47	-4.48	
$^3[\text{HNC}_2\text{NH}]^{2-}$ (m2)	$^1\text{NH} + ^1[\text{C}_2]^{2-} + ^3\text{NH}$	-10.79	-10.49	-9.67	-11.34(-11.35) ^a	-11.35	
	$^1\text{NH} + ^3[\text{C}_2]^{2-} + ^1\text{NH}$	-15.25	-14.96	-14.14	-14.36(-14.37) ^a	-14.37	
	$^3\text{NH} + ^3[\text{C}_2]^{2-} + ^3\text{NH}$	-10.88	-10.58	-9.71	-10.57(-10.58) ^a	-10.57	
$^3[\text{HNC}_2\text{NH}]^{2-}$ (m3)	$^1\text{NH} + ^1[\text{C}_2]^{2-} + ^3\text{NH}$	-7.62	-7.28	-6.45	-8.89	-8.89	
	$^1\text{NH} + ^3[\text{C}_2]^{2-} + ^1\text{NH}$	-12.08	-11.74	-10.92	-11.90	-11.91	
	$^3\text{NH} + ^3[\text{C}_2]^{2-} + ^3\text{NH}$	-7.71	-7.37	-6.48	-8.12	-8.12	
$^5[\text{HNC}_2\text{NH}]^{2-}$ (m1)	$^3\text{NH} + ^1[\text{C}_2]^{2-} + ^3\text{NH}$	-7.02	-6.71	-5.85	-8.14	-8.17	
	$^3\text{NH} + ^3[\text{C}_2]^{2-} + ^1\text{NH}$	-11.48	-11.18	-10.32	-11.16	-11.18	
$^5[\text{HNC}_2\text{NH}]^{2-}$ (m2)	$^3\text{NH} + ^1[\text{C}_2]^{2-} + ^3\text{NH}$	-3.40	-3.07	-2.21	-5.93	-5.94	
	$^3\text{NH} + ^3[\text{C}_2]^{2-} + ^1\text{NH}$	-7.86	-7.53	-6.68	-8.95	-8.95	
$^2[\text{C}_2\text{NH}]^-$ (m1)	$^2[\text{C}_2]^- + ^1\text{NH}$	-7.41	-7.27	-6.89	-6.81	-6.81	
	$^2[\text{C}_2]^- + ^3\text{NH}$	-5.22	-5.08	-4.68	-4.91	-4.91	
$^2[\text{HNC}_2\text{NH}]^-$ (m1)	$\text{C}_2 + ^2\text{NH}^-$	-9.19	-9.04	-8.67	-7.87	-7.84	
	$^2[\text{C}_2\text{NH}]^- + ^1\text{NH}$	-6.77	-6.59	-6.14	-6.31	-6.32	
	$^2[\text{C}_2\text{NH}]^- + ^3\text{NH}$	-4.58	-4.40	-3.92	-4.42	-4.42	
	$^1\text{NH} + ^2[\text{C}_2]^- + ^1\text{NH}$	-14.17	-13.85	-13.03	-13.12	-13.13	
	$^3\text{NH} + ^2[\text{C}_2]^- + ^1\text{NH}$	-11.99	-11.67	-10.82	-11.22	-11.23	
	$^3\text{NH} + ^2[\text{C}_2]^- + ^3\text{NH}$	-9.80	-9.48	-8.60	-9.33	-9.33	
	$^2\text{NH}^- + ^1\text{C}_2 + ^3\text{NH}$	-13.77	-13.44	-12.59	-12.29	-12.26	

^aAt the optimized RCCSD(T)/aug-cc-pVTZ geometry.

reaction energies with respect to the ground states of the in situ diatomic species $\text{C}_2(X^1\Sigma_g^+) + 2 \times \text{NH}(X^2\Pi) \rightarrow ^3[\text{HNC}_2\text{NH}]^{2-}$ (m1) is $-8.57[-8.53]$ eV at the CCSD(T) {QCISD(T)} methodologies, with respect to the $[\text{C}_2]^{2-}(X^1\Sigma_g^+) + 2 \times \text{NH}(X^3\Sigma^-) \rightarrow ^3[\text{HNC}_2\text{NH}]^{2-}$ (m1) is $-9.47[-9.48]$ eV, while for the reaction with respect to the

lowest in energy diatomic products $[\text{C}_2]^- (X^2\Sigma_g^+) + \text{NH}(X^3\Sigma^-) + \text{NH}^-(X^2\Pi) \rightarrow ^1[\text{HNC}_2\text{NH}]^{2-}$ (m1) is $-5.61[-5.61]$ eV, see Table 6.

Finally, MD calculations of the lowest energy singlet and triplet states of the $[\text{C}_2\text{NH}]^{2-}$ dianion and the triplet state of the $[\text{HNC}_2\text{NH}]^{2-}$ dianion were carried out via a classical

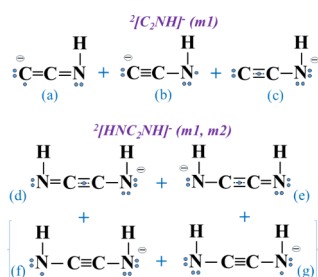
trajectory calculation using a Born–Oppenheimer molecular dynamics model at the B3LYP/6–311G+(d,p) level of theory. Starting from these minima structures, the molecules kept their structure, meaning that both are stable until 155 fs. The bond stretch toward the $[C_2\cdots NH]^{2-}$, $[C_2N\cdots H]^{2-}$, $[HNC_2\cdots NH]^{2-}$, and $[HNC_2N\cdots H]^{2-}$ bonds was investigated. In all cases, the m1 structures present the most stable potential energy. Furthermore, additional MD calculations were carried out, where the $[C_2\cdots NH]^{2-}$ and $[HNC_2\cdots NH]^{2-}$ distances were set as 2.0 Å. Regarding the $[C_2\cdots NH]^{2-}$, the m1 minima $[C_2NH]^{2-}$ dianion structures are stabilized after 18.6 fs (for the m1 singlet state) and 25.5 fs (for the m1 triplet state). On the contrary, regarding the $[HNC_2\cdots NH]^{2-}$ dianion, the system breaks to $[HNC_2]^{2-} + NH$; however, it is higher in energy than the m1 structure of the $[HNC_2NH]^{2-}$ dianion. It should be noted that the reason why the small bond stretch does not break the $[C_2NH]^{2-}$ and $[HNC_2NH]^{2-}$ is that either the $[C_2]^-$ or the C_2 group that is stable is involved in the bonding.

3.3. $[C_2NH]^-$ and $[HNC_2NH]^-$

The electronic and molecular structures of the $[C_2NH]^-$ and $[HNC_2NH]^-$ anions, see Figure 2, were studied to calculate their electron affinity. The electron detachment of the $[C_2]^{2-}$, $[C_2NH]^{2-}$, and $[HNC_2NH]^{2-}$ dianions is calculated at 3.62, 3.54, and 3.48 eV, respectively, showing that the addition of each NH reduces it by 0.06 eV. Note that MD simulations have shown that both dianions, since they formed, can remain for enough time so as to be experimentally observed.

Regarding their bonding, in $[C_2NH]^-$ the charge is distributed in the remote C atom and in the N atom, while the central C atom is in the 5S excited state. So, three configurations are possible. Note that the (a) and (b) configurations correspond to the same diatomic reactants $[C_2]^- + NH$, while the (c) configuration corresponds to $C_2 + NH^-$. We can consider that the bonding is described by the (a) and (b) configurations because both populations show that the charge in the remote C atom is larger than the charge in the N atom. In the $[HNC_2NH]^-$ anion, as in the case of the $[HNC_2NH]^{2-}$ anion, both C atoms are in their 5S excited state, while the charge is distributed to the N atoms, see Scheme 3. Thus, the (d) and (e) configurations equally

Scheme 3. Chemical Bonding of the $^2[C_2NH]^-$ and $^2[HNC_2NH]^-$ Dianions



contribute to the bonding. They differ in which nitrogen is negatively charged. The (f) and (g) configurations differ from the (d) and (e) ones in which atom C or N has the unpaired electron. While the unpaired electron is distributed to the whole molecule, the density is more intense at the center than at the remote atoms; therefore, the (d) and (e) configurations are the favored ones. Furthermore, the short N–C bond

distance of 1.309 Å is in accordance with the formation of a 1.5 bond on average, see Scheme 3.

The reaction energies with respect to the lowest in energy diatomic products are -4.91 eV for the reaction $[C_2]^- (X^2\Sigma_g^+) + NH(X^3\Sigma^-) \rightarrow ^2[C_2NH]^-$ (m1) and -9.33 eV for the reaction $[C_2]^- (X^2\Sigma_g^+) + NH(X^3\Sigma^-) + NH^-(X^2\Pi) \rightarrow ^2[HNC_2NH]^-$ (m1) at the CCSD(T) method. Finally, formation reaction of the $[HNC_2NH]^-$ from $[C_2NH]^-$, i.e., $^2[C_2NH]^- + NH(X^3\Sigma^-) \rightarrow ^2[HNC_2NH]^-$ is -4.42 eV, similar to the value of -4.47 eV for the addition of the $NH(X^3\Sigma^-)$ to the $^2[C_2NH]^{2-}$, see Table 6.

3.4. Comparison N_2NH and HNN_2NH vs $[C_2NH]^{2-}$ and $[HNC_2NH]^{2-}$

In general, all methodologies used, namely B3LYP, CCSD(T), QCISD(T), MRCISD and MRCISD+Q predict similar energetics regarding reaction energies and relative ordering of the structures, except for $[C_2NH]^{2-}$, i.e., B3LYP predicts a singlet structure lower in energy than a triplet one; however, their B3LYP energy difference is only 0.33 eV. Multireference methods also predict the triplet one as the lowest in energy; however, their energy difference is only 0.03 eV.

The N_2 and $[C_2]^{2-}$ species are isoelectronic, and even though both form a triple bond in their $X^1\Sigma_g^+$ state, and a double bond in their first excited $A^3\Sigma_u^+$ state, the $A^3\Sigma_u^+$ lies higher than the X state at 6.2 eV in N_2 , and only at 1.1 eV in $[C_2]^{2-}$. Thus, their binding energies and relative stability differ. These differences, along with the metastable nature of $[C_2]^{2-}$, influence the binding energy, the relative stability, and the bonding of the N_2NH , HNN_2NH , $[C_2NH]^{2-}$, and $[HNC_2NH]^{2-}$ species.

Thus, both N_3H and N_4H_2 molecules present singlet spin ground states, while both $[C_2NH]^{2-}$ and $[C_2N_2H_2]^{2-}$ dianions present triplet spin ground states, for the $[C_2NH]^{2-}$ dianion, both singlet and triplet states are almost energetically degenerate. In both molecules, the attachment of the second NH to the X_2NH can affect the bonding of the X_2 , NH, and X_2-NH , and the charge of the X_2 species, where $X = N$ or C^- .

In Figure 5, the reaction energies of the (a) $2 \times NH + N_2 \rightarrow HNN_2NH \rightarrow N_2NH + NH \rightarrow 2 \times NH + N_2$ and (b) $2 \times NH + [C_2]^{2-} \rightarrow [HNC_2NH]^{2-} \rightarrow [C_2NH]^{2-} + NH \rightarrow 2 \times NH + [C_2]^{2-}$ reactions at the CCSD(T)/aug-cc-pVTZ level of theory are presented to show the difference observed in both systems, i.e., N_2NH vs $[C_2NH]^{2-}$ and HNN_2NH vs $[HNC_2NH]^{2-}$. Thus, the reaction $HNN_2NH \rightarrow N_2NH + NH$ is less demanding than the $[HNC_2NH]^{2-} \rightarrow [C_2NH]^{2-} + NH$ due to the fact that the bonding change in the central N_2 during the attachment of the second NH, while in the case of the $[C_2]^{2-}$, does not change. Specifically, in the N_2NH , the $N \equiv N$ is involved and in HNN_2NH the $=N-N=$, while in both $[HNC_2NH]^{2-}$ and $[C_2NH]^{2-}$ the $C-C$ bonding is similar, i.e., a triple " $C \equiv C$ " bond in both singlet states and a double " $C=C$ " bond in both triplet states.

Furthermore, even though $[C_2]^{2-}$ has been observed, it is metastable due to an autodetachment process, where an autoionization process occurs, and the electron is spontaneously emitted. The $[C_2]^-$ is more stable than $[C_2]^{2-}$ by 3.62 eV, while the $NH^-(X^2\Pi)$ is more stable than NH by 0.23 eV at the CCSD(T)/aug-cc-pVTZ. So, the $[C_2]^{2-}$ does not be retained in the $[C_2NH]^{2-}$ and $[C_2N_2H_2]^{2-}$ dianions; specifically in the $[C_2NH]^{2-}$, the $[C_2]^-$ is involved with a triplet bonding in the case of $^1[C_2NH]^{2-}$ and a double in the case of the $^3[C_2NH]^{2-}$, while when a second NH is added, the

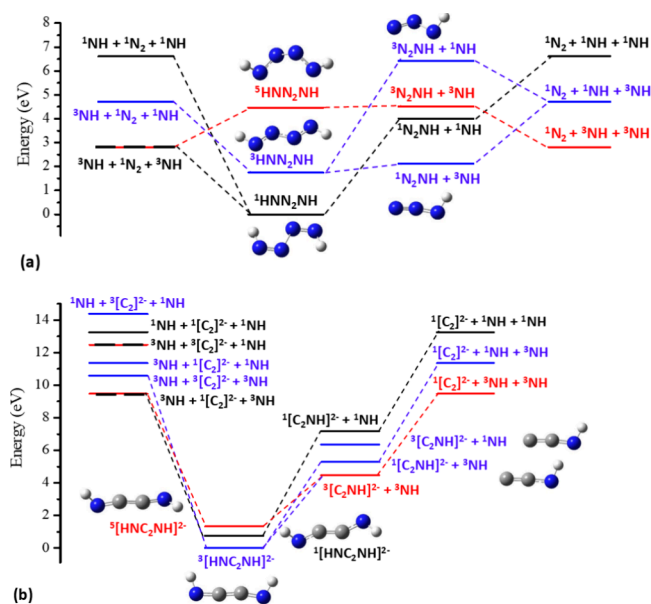


Figure 5. Reaction energies of: (a) $2 \times \text{NH} + \text{N}_2 \rightarrow \text{HNN}_2\text{NH} \rightarrow \text{N}_2\text{NH} + \text{NH} \rightarrow 2 \times \text{NH} + \text{N}_2$ and (b) $2 \times \text{NH} + [\text{C}_2]^{2-} \rightarrow [\text{HNC}_2\text{NH}]^{2-} \rightarrow [\text{C}_2\text{NH}]^{2-} + \text{NH} \rightarrow 2 \times \text{NH} + [\text{C}_2]^{2-}$ reactions at the CCSD(T)/aug-cc-pVTZ level of theory.

C_2 is involved with a triplet bonding in the case of $^1[\text{HNC}_2\text{NH}]^{2-}$ and a double in the case of the $^3[\text{HNC}_2\text{NH}]^{2-}$. In all cases, the C (^5S) atomic state is involved.

Finally, the X–X and N–H bond distances of X_2NH and HNX_2NH , where X = N and C^- , reflect the geometries of the corresponding diatomic fragments. Comparing the global minimum of the X_2NH species, namely, $^1\text{N}_2\text{NH}$ (m1), $^3[\text{C}_2\text{NH}]^{2-}$ (m1), and $^2[\text{C}_2\text{NH}]^-$, the $^1\text{N}_2\text{NH}$ structure has a X–X bond distance of 1.136 Å, whereas the $^3[\text{C}_2\text{NH}]^{2-}$ and $^2[\text{C}_2\text{NH}]^-$ species exhibit elongated X–X bond distances by about 0.15 Å. The N–H bond distances in these three species are similar, while the X–N bond distance is approximately 0.06 longer when X is C or C^- . Comparing the geometries of $^1\text{HNN}_2\text{NH}$ (m1), $^3\text{HNN}_2\text{NH}$ (m1), $^3[\text{HNC}_2\text{NH}]^{2-}$ (m1), and $^2[\text{HNC}_2\text{NH}]^-$ (m1), the first one presents an elongated X–X bond distance of 1.439 Å, corresponding to a single bond. In contrast, the remaining species display significantly shorter X–X bond distances, consistent with multiple bonding. Specifically, the X–X bond distance is 1.293 Å for the $^3\text{HNN}_2\text{NH}$, while both $^3[\text{HNC}_2\text{NH}]^{2-}$ and $^2[\text{HNC}_2\text{NH}]^-$ exhibit the same shorter distance of about 1.253 Å. Finally, it is worth noting that both $^3[\text{C}_2\text{NH}]^{2-}$ and $^2[\text{C}_2\text{NH}]^-$ possess similar geometries as do $^3[\text{HNC}_2\text{NH}]^{2-}$ and $^2[\text{HNC}_2\text{NH}]^-$.

4. CONCLUSIONS

In the present study, the electronic and molecular structure, the chemical bonding, and thermochemical stability of the N_3H and N_4H_2 molecules and of the isoelectronic $[\text{C}_2\text{NH}]^{2-}$ and $[\text{C}_2\text{N}_2\text{H}_2]^{2-}$ anions are studied via DFT, CCSD(T), QCISD(T), and MRCISD methodologies. Their dissociation energies with respect to $\text{HN} + \text{N}_2$, $\text{HN} + \text{C}_2^{2-}$, $\text{HN} + \text{C}_2^-$, $\text{HN}^- + \text{C}_2^{2-}$ and $\text{HN}^- + \text{C}_2^-$ moieties are calculated, and potential energy curves were plotted. The energetics of the reaction are gathered in Figure 6 and the reaction enthalpies

with respect to the correlated diatomic products, and the in situ diatomic molecules are listed in Table 7.

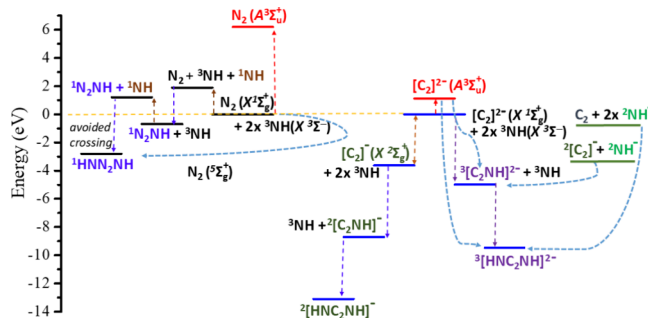


Figure 6. Reaction energies of the $2 \times \text{NH} + \text{N}_2 \rightarrow \text{N}_2\text{NH} + \text{NH} \rightarrow \text{HNN}_2\text{NH}$, $2 \times \text{NH} + [\text{C}_2]^{2-} \rightarrow [\text{C}_2\text{NH}]^{2-} + \text{NH} \rightarrow [\text{HNC}_2\text{NH}]^{2-}$, $\text{NH}^- + [\text{C}_2]^- \rightarrow [\text{C}_2\text{NH}]^{2-}$, and $2 \times \text{NH}^- + \text{C}_2 \rightarrow [\text{HNC}_2\text{NH}]^{2-}$ reactions at the CCSD(T)/aug-cc-pVTZ level of theory.

Both N_2 and $[\text{C}_2]^{2-}$ species are isoelectronic; they present the same ground and first excited state, forming the same bonds; however, their binding energies and relative stability differ. These differences, along with the metastable nature of $[\text{C}_2]^{2-}$, influence the binding energy and bonding of the N_2NH , HNN_2NH , $[\text{C}_2\text{NH}]^{2-}$, and $[\text{HNC}_2\text{NH}]^{2-}$ species. Thus, both N_2NH and HNN_2H molecules present singlet spin ground states, while both $[\text{C}_2\text{NH}]^{2-}$ and $[\text{C}_2\text{N}_2\text{H}_2]^{2-}$ anions present triplet spin ground states, while in the case of $[\text{C}_2\text{NH}]^{2-}$, the singlet state is almost energetically degenerate with the triplet one.

In the $\text{N}\equiv\text{N}-\text{NH}$ molecule, the $\text{N}_2(X^1\Sigma_g^+)$ forms a triple bond, the NH is excited at the $a^1\Delta$ state, while a dative bond is formed from the N_2 to N of the NH ($a^1\Delta$). On the contrary, the $\text{HN}=\text{N}-\text{N}=\text{NH}$ has a central $\text{N}_2(^5\Sigma_g^+)$ molecule having a single bond, while the two NH molecules are in their ground state ($X^3\Sigma^-$), and double bonds are formed between the N atoms of N_2 and the NH molecules. Thus, the addition of the second NH molecule affects the bonding of the N_2 . The reaction energies of the $\text{NH}(a^1\Delta) + \text{N}_2(X^1\Sigma_g^+) \rightarrow \text{N}_2\text{NH}$ are calculated at -2.59 eV at RCCSD(T). Finally, the $^1\text{HNN}_2\text{NH}$ (m1 and m2), contains an excited state of $\text{N}_2(^5\Sigma_g^+)$ located 9.17 eV above its ground $\text{N}_2(X^1\Sigma_g^+)$ state, with four unpaired p electrons that form two covalent bonds with the $\text{NH}(X^3\Sigma^-)$. The m1 and m2 are stable with respect to the ground state diatomic molecules, and the formation energy with respect to them is -2.83 eV at RCCSD(T), while with respect to the in situ diatomic products, it is increased to -11.93 eV.

In the $[\text{C}_2\text{NH}]^{2-}$ anion, one electron is transferred from $[\text{C}_2]^{2-}$ to the NH, and the bonding is formed between $[\text{C}_2]^- + \text{NH}^-$, i.e., the charges are located at the N atom and the outer C atom. In $[\text{HNC}_2\text{NH}]^{2-}$ the bonding is formed among $2 \times \text{NH}^- + \text{C}_2$. In the singlet states of the $[\text{C}_2\text{NH}]^{2-}$ and $[\text{HNC}_2\text{NH}]^{2-}$ anions, triple bonds are formed in $[\text{C}_2]^-$ and C_2 , respectively. For the triplet state of the $[\text{C}_2\text{NH}]^{2-}$ anion, its formation energy with respect to the lowest ground state species $[\text{C}_2]^- (X^3\Sigma_g^+) + \text{NH}^- (X^2\Pi) \rightarrow ^3[\text{C}_2\text{NH}]^{2-}$ (m1) is -1.14 eV, while for the reaction $[\text{C}_2]^{2-} (X^1\Sigma_g^+) + \text{NH}(X^3\Sigma^-) \rightarrow ^3[\text{C}_2\text{NH}]^{2-}$ (m1) is -4.99 eV at the CCSD(T) method. For the triplet state of the $[\text{HNC}_2\text{NH}]^{2-}$ anion, the reaction energies with respect to the ground states of the in situ diatomic species is, $\text{C}_2(X^1\Sigma_g^+) + 2 \times \text{NH}^- (X^2\Pi) \rightarrow ^3[\text{HNC}_2\text{NH}]^{2-}$ (m1) is -8.57 eV, while for the reaction

Table 7. Reaction Enthalpies ΔH_r (eV) of the Calculated reactions^a and In Situ Diatomics at B3LYP/6–311+G(d,p), CCSD(T) and QCISD(T)/aug-cc-pVTZ Methods

reaction ^a	B3LYP	CCSD(T)	QCISD(T)	in situ diatomics
$\text{NH}(a^1\Delta) + \text{N}_2(X^1\Sigma_g^+) \rightarrow {}^1\text{N}_2\text{NH}$	−2.98	−2.43	−2.45	$\text{NH}(a^1\Delta) + \text{N}_2(X^1\Sigma_g^+)$
$2 \times \text{NH}(X^3\Sigma^-) + \text{N}_2(X^1\Sigma_g^+) \rightarrow {}^1\text{HNN}_2\text{NH}$	−2.60	−2.44	−2.45	$2 \times \text{NH}(X^3\Sigma^-) + \text{N}_2(X^1\Sigma_g^+)$
$\text{NH}(X^3\Sigma^-) + [\text{C}_2]^{2-}(X^1\Sigma_g^+) \rightarrow {}^3[\text{C}_2\text{NH}]^{2-}$	−3.80	−4.85	−4.86	$\text{NH}^-(X^2\Pi) + [\text{C}_2]^-$
$2 \times \text{NH}(X^3\Sigma^-) + [\text{C}_2]^{2-}(A^3\Sigma_u^+) \rightarrow {}^3[\text{C}_2\text{N}_2\text{H}_2]^{2-}$	−8.30	−9.16	−9.17	$2 \times \text{NH}^-(X^2\Pi) + \text{C}_2$

^aMultiplicity of spin is provided as superscript at the left of each compound.

with respect to the lowest in energy diatomic products, is $[\text{C}_2]^- (X^2\Sigma_g^+) + \text{NH}(X^3\Sigma^-) + \text{NH}^-(X^2\Pi) \rightarrow {}^1[\text{HNC}_2\text{NH}]^{2-}$ (m1) is −5.61 eV, Table 6.

Finally, while the $[\text{C}_2]^{2-}$ dianion is metastable, the attachment of one NH stabilizes it, i.e., both dianions $[\text{C}=\text{C}-\text{NH}]^{2-}$ and $[\text{HN}-\text{C}=\text{C}-\text{NH}]^{2-}$ are stable with respect to the ground states of $[\text{C}_2]^-$ and NH by 1.37 and 5.85 eV, respectively. The electron detachment of the $[\text{C}_2]^{2-}$ dianion is 3.62 eV, while the addition of one NH reduces it to 3.54 eV, and the addition of the second NH further reduces it to 3.48 eV. MD simulations show that both dianions, since they formed, can remain for enough time so as to be experimentally observed.

The present research not only predicts that the dianions $[\text{C}_2\text{NH}]^{2-}$ and $[\text{HNC}_2\text{NH}]^{2-}$ can be formed and remain long enough for experimental observation but also provides useful information on the bonding of polynitrogen systems, their reactivity, and their stability. The present results can provide deeper chemical insights into nitrogen chemistry, while the potential roles of the calculated species in nitrogen fixation or nitrogen chemistry can be further investigated. Overall, the present study can be extended in several ways in future work. Specifically, future experimental validation of the formation of the dianions can be conducted to confirm our theoretical predictions. Furthermore, dynamical and spectroscopic studies can further investigate the dynamics, vibrational spectra, and electronic spectra of these species. Additionally, extended computations on larger polynitrogen systems related to these moieties could be explored to understand how bonding and electronic properties evolve with system size. Their potential roles in nitrogen fixation or nitrogen chemistry, and detailed mechanistic pathways of formation and decomposition, can provide deeper chemical insights. Finally, this study can be further expanded to other isoelectronic systems, such as those involving carbon–nitrogen or carbon–carbon species with similar bonding motifs, which could highlight broader principles governing stability and bonding differences. These directions would advance the chemical understanding of these isoelectronic moieties and related species, exploring potential applications in materials science or nitrogen chemistry.

■ ASSOCIATED CONTENT

SI Supporting Information

The Supporting Information is available free of charge at <https://pubs.acs.org/doi/10.1021/acsomega.5c09124>.

Geometries, Mulliken and NPA population analysis, valence molecular orbitals, and classical molecular dynamics trajectories of the X_2NH and HNX_2NH , where $\text{X} = \text{N}$ and C^- , C (PDF)

■ AUTHOR INFORMATION

Corresponding Author

Demeter Tzeli – Department of Chemistry, National and Kapodistrian University of Athens, Athens 157 71, Greece; Theoretical and Physical Chemistry Institute, National Hellenic Research Foundation, Athens 116 35, Greece; orcid.org/0000-0003-0899-7282; Email: tzeli@chem.uoa.gr

Author

Georgios A. Tsekouras – Department of Materials Science & Engineering, University of Ioannina, Ioannina 451 10, Greece

Complete contact information is available at: <https://pubs.acs.org/doi/10.1021/acsomega.5c09124>

Funding

The open access publishing of this article is financially supported by HEAL-Link.

Notes

The authors declare no competing financial interest.

■ ACKNOWLEDGMENTS

HEAL-Link is acknowledged for financial support of the open access publishing of this article.

■ REFERENCES

- (1) Yao, Y.; Adeniyi, A. O. Solid nitrogen and nitrogen-rich compounds as high-energy-density materials. *Phys. Status Solidi B* **2021**, *258*, No. 2000588.
- (2) (a) Wang, Y.; et al. Stabilization of hexazine rings in potassium polynitride at high pressure. *Nat. Chem.* **2022**, *14*, 794–800. (b) Ninet, S. Benzene-like N₆ hexazine rings. *Nat. Chem.* **2023**, *15*, 595–596. (c) Qian, W.; Marduykov, A.; Schreiner, P. R. Preparation of a neutral nitrogen allotrope hexanitrogen C₂h-N₆. *Nature* **2025**, *642*, 356–360.
- (3) Christe, K. O. Polynitrogen chemistry enters the ring. *Science* **2017**, *355*, 351–351.
- (4) Betterton, E. A. Environmental fate of sodium azide derived from automobile airbags. *Crit. Rev. Environ. Sci. Technol.* **2003**, *33*, 423–458.
- (5) Orlando, J. J.; Tyndall, G. S.; Betterton, E. A.; Lowry, J.; Stegall, S. Atmospheric Chemistry of Hydrazoic Acid (HN₃): UV Absorption Spectrum, HO[•] Reaction Rate, and Reactions of the [•]N₃ Radical. *Environ. Sci. Technol.* **2005**, *39*, 1632–1640.
- (6) Glukhovtsev, M. N.; Bach, R. D.; Laiter, S. S. High-Level Computational Study on the Thermochemistry of Saturated and Unsaturated Three- and Four-Membered Nitrogen and Phosphorus Rings. *Int. J. Quantum Chem.* **1997**, *62*, 373–384.
- (7) Karahodza, A.; Knaus, K. J.; Ball, D. W. Cyclic triamines as potential high energy materials. Thermochemical properties of triaziridine and triazirine. *J. Mol. Struct.: THEOCHEM* **2005**, *732*, 47–53.

- (8) Furman, D.; Dubnikova, F.; van Duin, A. C. T.; Zeiri, Y.; Kosloff, R. Reactive Force Field for Liquid Hydrazoic Acid with Applications to Detonation Chemistry. *J. Phys. Chem. C* **2016**, *120*, 4744–4752.
- (9) Glukhovtsev, M. N.; Laiter, S. Thermochemistry of Tetrazete and Tetraazetetrahedrane: A High-Level Computational Study. *J. Phys. Chem.* **1996**, *100*, 1569–1577.
- (10) (a) Samanta, S.; Das, S.; Biswas, P. Photocatalysis by 3,6-Disubstituted-s-Tetrazine: Visible-Light Driven Metal-Free Green Synthesis of 2-Substituted Benzimidazole and Benzothiazole. *J. Org. Chem.* **2013**, *78*, 11184–11193. (b) Mondal, J.; Sivaramakrishna, A. Functionalized Triazines and Tetrazines: Synthesis and Applications. *Top. Curr. Chem.* **2022**, *380*, 34.
- (11) (a) Rosso, C.; Withnall, R.; Kjaergaard, H. G.; Taylor, R. A.; Helm, H.; Mordaunt, D. H.; Fielding, H. H. Electronic and Vibrational Absorption Spectra of NH₂ in Solid Xenon Matrix. *ACS Omega* **2019**, *4*, 3959–3967. (b) Newcomb, M.; Dey, C. C.; Yadava, B. R. The Stability of Nitrogen-Centered Radicals. *Org. Biomol. Chem.* **2015**, *13*, 1234–1246. (c) Hari, D. P.; König, B. Nitrogen-Centered Radicals in Functionalization of sp² Systems: Generation, Reactivity, and Applications in Synthesis. *Chem. Rev.* **2022**, *122*, 8181–8260. (d) Guo, J.; Zhang, J.; Su, H.; Xu, T.; Wei, D.; Zhang, Y.; Yang, C. Neutral Stable Nitrogen-Centered Radicals: Structure, Properties, and Recent Functional Application Progress. *Adv. Funct. Mater.* **2025**, *35*, No. 2304291. (e) DePrince, A. E., III; Shafiei, A.; Loipersberger, M.; Dyall, K. G. Design of an Open-Shell Nitrogen-Centered Diradicaloid: Electronic Structure and Properties. *J. Phys. Chem. Lett.* **2022**, *13*, 4356–4363. (f) Laeber, K. F. P.; Uhlig, F.; Colombo, L.; Greb, L. Theoretical Studies of Nitrogen Doped Polycyclic Aromatic Hydrocarbons: Electronic Structure and CO₂ Physisorption. *J. Phys. Chem. A* **2025**, *129*, 4567–4578. (g) Chu, K.; Wang, R.; Sun, Y.; Li, G.; Kwon, Y.; Al-Enizi, A. M.; Yu, J.; Liu, H. Catalysts and Reaction Environments in Electrochemical Nitrogen Reduction: Mechanisms and Efficiency. *Chem. Rev.* **2025**, *125*, 842–888.
- (12) Weltner, W., Jr.; Van Zee, R. J. Carbon molecules, ions, and clusters. *Chem. Rev.* **1989**, *89*, 1713.
- (13) Honig, R. E. Mass Spectrometric Study of the Molecular Sublimation of Graphite. *J. Chem. Phys.* **1954**, *22*, 126–131.
- (14) Schauer, S. N.; Williams, P.; Compton, R. N. Production of small doubly charged negative carbon cluster ions by sputtering. *Phys. Rev. Lett.* **1990**, *65*, 625.
- (15) Mathur, D.; Bhardwaj, V. R.; Rajgara, F. A.; Safvan, C. P. Search for doubly charged negative ions of small carbon clusters. *Chem. Phys. Lett.* **1997**, *277*, 558–563.
- (16) Pedersen, H. B.; Djuric, N.; Jensen, M. J.; Kella, D.; Safvan, C. P.; Vejby-Christensen, L.; Andersen, L. H. Doubly Charged Negative Ions of B₂ and C₂. *Phys. Rev. Lett.* **1998**, *81*, 5302–5305.
- (17) Watts, J. D.; Bartlett, Rodney J. A theoretical study of linear carbon cluster monoanions, C_n⁻, and dianions, C_n²⁻ (n = 2–10). *J. Chem. Phys.* **1992**, *97*, 3445–3457.
- (18) Sommerfeld, T.; Riss, U. V.; Meyer, H.-D.; Cederbaum, L. S. Metastable C₂⁻² Dianion. *Phys. Rev. Lett.* **1997**, *79*, 1237.
- (19) Sommerfeld, T.; Tarantelli, F.; Meyer, H.-D.; Cederbaum, L. S. Ab initio calculation of energies and lifetimes of metastable dianions: The resonance. *J. Chem. Phys.* **2000**, *112*, 6635–6642.
- (20) Lee, C. T.; Yang, W. T.; Parr, R. G. Development of the Colle-Salvetti correlation energy formula into a functional of the electron density. *Phys. Rev. B: Condens. Matter Mater. Phys.* **1988**, *37*, 785–789.
- (21) Becke, A. D. A new mixing of hartree-fock and local density-functional theories. *J. Chem. Phys.* **1993**, *38*, 1372–1377.
- (22) Curtiss, L. A.; McGrath, M. P.; Blauddau, J. P.; Davis, N. E.; Binning, R. C.; Radom, L. Extension of gaussian-2 theory to molecules containing third-row atoms Ga-Kr. *J. Chem. Phys.* **1995**, *103*, 6104–6113.
- (23) Li, X.; Millam, J. M.; Schlegel, H. B. Ab initio molecular dynamics studies of the photodissociation of formaldehyde, H₂CO → H₂+CO: Direct classical trajectory calculations by MP2 and density functional theory. *J. Chem. Phys.* **2000**, *113*, 10062–10067.
- (24) Thompson, D. L., in *Encyclopedia of Computational Chemistry*; Schleyer, P. v. R.; Allinger, N. L.; Kollman, P. A.; Clark, T.; Schaefer, H. F., III; Gasteiger, J.; Schreiner, P. R.; Wiley: Chichester, 1998; pp 3056–3073
- (25) Uggerud, E.; Helgaker, T. Dynamics of the Reaction CH₂OH⁺ → CHO⁺ + H₂. Translational Energy-Release from ab initio Trajectory Calculations. *J. Am. Chem. Soc.* **1992**, *114*, 4265–4268.
- (26) Purvis, G. D.; Bartlett, R. J. A full coupled-cluster singles and doubles model: The inclusion of disconnected triples. *J. Chem. Phys.* **1982**, *76*, 1910–1918.
- (27) Deegan, M. J. O.; Knowles, P. J. Perturbative corrections to account for triple excitations in closed and open-shell coupled-cluster theories. *Chem. Phys. Lett.* **1994**, *227*, 321–326.
- (28) Pople, J. A.; Head-Gordon, M.; Raghavachari, K. Quadratic configuration interaction – a general technique for determining electron correlation energies. *J. Chem. Phys.* **1987**, *87*, 5968–5975.
- (29) Salter, E. A.; Trucks, G. W.; Bartlett, R. J. Analytic Energy Derivatives in Many-Body Methods. I. First Derivatives. *J. Chem. Phys.* **1989**, *90*, 1752–1766.
- (30) (a) Dunning, T. H. Gaussian-basis sets for use in correlated molecular calculations. I. The atoms boron through neon and hydrogen. *J. Chem. Phys.* **1989**, *90*, 1007–1023. (b) Kendall, R. A.; Dunning, T. H.; Harrison, R. J. Electron-affinities of the first-row atoms revisited. Systematic basis-sets and wave-functions. *J. Chem. Phys.* **1992**, *96*, 6796–6806.
- (31) (a) He, X.; Ervin, K. M.; McCoy, A. B.; Lineberger, W. C. Accurate Benchmark Calculations on the Gas-Phase Acidities of Small Molecules: Evidence that CCSD(T)/aug-cc-pVTZ Energies Are Close to the Complete Basis Set Limit. *J. Phys. Chem. A* **2009**, *113*, 5801–5807. (b) Sirirak, J.; Perry, J. S. A.; Boatz, J. R.; Furness, J. W.; Lopez, S. A.; Leverentz, H. R.; Allen, W. D.; Scuseria, G. E.; Schultz, A. J.; Gwaltney, S. R. Benchmarking Quantum Mechanical Methods for Reaction Energies of Small Organic Molecules: Accuracy of CCSD(T)/aug-cc-pVTZ for Reaction Energy Calculations. *PeerJ. Phys. Chem.* **2020**, *2*, No. e100. (c) Tzeli, D.; Mato, J.; Xantheas, S. S. The many-body expansion for metals: II. Non-additive terms in clusters comprised of metals with ns¹, ns² and ns²p¹ configurations. *J. Phys. Chem. A* **2025**, *129*, 3648.
- (32) Langhoff, S. R.; Davidson, E. R. Configuration interaction calculations on the nitrogen molecule. *Int. J. Quantum Chem.* **1974**, *8*, 61–72.
- (33) (a) Werner, H.-J.; Knowles, P. J. An efficient internally contracted multiconfiguration–reference configuration interaction method. *J. Chem. Phys.* **1988**, *89*, 5803–5814. (b) Werner, H.-J.; Reinsch, E. A. The self-consistent electron pairs method for multiconfiguration reference state functions. *J. Chem. Phys.* **1982**, *76*, 3144–3156.
- (34) (a) King, D.; Szalay, P. G.; Tait, C. E.; Gagliardi, L. Large-Scale Benchmarking of Multireference Vertical Excitation Energies with aug-cc-pVTZ Basis Set. *J. Chem. Theory Comput.* **2022**, *18*, 8003–8016. (b) Tzeli, D.; Raugei, S.; Xantheas, S. S. Quantitative Account of the Bonding Properties of a Rubredoxin Model Complex [Fe(SCH₃)₄]^q, q = −2, −1, +2, +3. *J. Chem. Theory Comput.* **2021**, *17*, 6080–6091.
- (35) Frisch, M. J.; Trucks, G. W.; Schlegel, H. B.; Scuseria, G. E.; Robb, M. A.; Cheeseman, J. R.; Scalmani, G.; Barone, V.; Mennucci, B.; Petersson, G. A. et al. *Gaussian 16, Revision C.01*; Gaussian, Inc.: Wallingford, CT, USA, 2016.
- (36) Werner, H.-J.; Knowles, P. J.; Manby, F. R.; Black, J. A.; Doll, K.; Heßelmann, A.; Kats, D.; Köhn, A.; Korona, T.; Kreplin, D. A.; et al. MOLPRO version 2022; The Molpro quantum chemistry package. *J. Chem. Phys.* **2020**, *152*, No. 144107.
- (37) Huber, K. P.; Herzberg, G., *Molecular Spectra and Molecular Structure. Constants of Diatomic Molecules*; van Nostrand Reinhold: New York, 1979.
- (38) (a) Feldmann, D.; Naturforsch, Z. Teil A **1970**, *25*, 621. (b) Feldmann, D.; Rackwitz, R.; Heinicke, E.; Kaiser, H. J. Electron affinities of some elements. *Phys. Lett. A* **1973**, *45*, 404.
- (39) (a) Jones, P. L.; Mead, R. D.; Kohler, B. E.; Rosner, S. D.; Lineberger, W. C. Photodetachment spectroscopy of C₂⁻ autodetaching resonances. *J. Chem. Phys.* **1980**, *73*, 4419. see also (b) Nichols, J.

A.; Simons, J. Theoretical study of C_2 and C_2^- : $X^1\Sigma^+$, $a^3\Pi_u$, $X^2\Sigma^+$, and $B^2\Sigma^+$ potentials. *J. Chem. Phys.* **1987**, *86*, 6972.

(40) Ervin, K. M.; Lineberger, W. C. Photoelectron spectra of C_2^- and C_2H^- . *J. Phys. Chem.* **1991**, *45*, 1167.

(41) Buchowiecki, M.; Szabo, P. N–H collision integrals with study of repulsive interactions *Plasma Sources Sci. Technol.* **2022**, *31*, No. 045010.

(42) Tzeli, D.; Xantheas, S. S. Breaking Covalent Bonds in the Context of the Many-Body Expansion (MBE): I. The purported "first row anomaly" in XH_n ($X = C, Si, Ge, Sn$; $n = 1-4$). *J. Chem. Phys.* **2022**, *156*, No. 244303.



CAS INSIGHTS™

EXPLORE THE INNOVATIONS SHAPING TOMORROW

Discover the latest scientific research and trends with CAS Insights. Subscribe for email updates on new articles, reports, and webinars at the intersection of science and innovation.

Subscribe today

CAS
A Division of the
American Chemical Society